UNIVERSITY OF CALIFORNIA SAN DIEGO

MIMO Process Control for Compressor Systems with Recycled Flow

A Thesis submitted in partial satisfaction of the requirements
for the degree Master of Science

in

Engineering Sciences (Mechanical Engineering)

by

Varun Ramadurai

Committee in charge:

Professor Robert Bitmead, Chair
Professor Raymond A de Callafon
Professor Mamadou Diagne

2024

The Thesis of Varun Ramadurai is approved, and it is acceptable in quality and form for publication on microfilm and electronically.

University of California San Diego

2024

TABLE OF CONTENTS

LIST OF FIGURES

LIST OF TABLES

LIST OF ABBREVIATIONS

MIMO	Multi Input Multi Output
SISO	Single Input Single Output
PID	Proportional Integral Derivative
LTI	Linear Time Invariant
ASV	Anti Surge Valve
EMD	Electric Motor Drive
GCTF	Gas Compressor Test Facility
AAF	Anti-Aliasing Filter
PSIG	Pounds per Square Inch Gauge
CARE	Continuous time Algebraic Riccati Equation

ACKNOWLEDGEMENTS

This section was left as the last part to be completed in this thesis, thinking it would take but a few minutes to finish it. How wrong I was to underestimate the difficulty of writing acknowledgments. Not because of the formal language or the correct etiquette to be followed, but because writing an acknowledgment forces you to introspect on the whole journey and humbly accept that there would not be anything to write about in the first place if it wasn't for the love, sacrifice, support and guidance from the people in your life.

I would truly like to acknowledge and thank Professor Robert Bitmead for his support and guidance through the tempest that is graduate school. What makes his counsel even more impressive is that we weren't even in the same continent for most of it. Knowing that he would have to stay late into the evening in his office at Stuttgart made our (my) 7am meetings on Mondays slightly easier to wake up to. As every advisor does, he has had an immeasurable impact on my academic development; but given his enormous success as a researcher, it is his humbleness, sense of humor and his ability to connect with people that has left a lasting impression on me. I would be remiss if I did not acknowledge the other members of my committee: Professor Raymond de Callafon and Professor Mamadou Diagne. From fighting the department for TA'ships to simply giving me their time to hear out my thoughts, I am truly thankful for their support as well.

The efforts and sacrifices it took to for me to even get to UCSD cannot be forgotten. My parents and sister, my biggest supporters, for their unwavering belief in me and supporting my decision to move across the world as a naïve undergrad despite the burden on them. I definitely cannot forget the friends I was lucky enough to make on my journey, who continue to inspire me to push forward every day and be the best version of myself. Brad

Ratto and Kwang-Hak Kim: for sharing in all my joys and disappointments, companionship, advice, countless favors without question, and the incredible memories we've made outside of work (and most importantly for a desk in their lab so I wouldn't have to be alone in mine). Evelia whose, presence in the lab would always brighten my day. Cenk, for being my walking controls encyclopedia and the career advice you've given me. Arthi and Eliana, for patiently helping me adjust to life in a new country and culture. Tim, who kept me sane and relaxed by always being ready to go out and play any sport at a moment's notice. And last but definitely the most impactful on my mental health, the dogs Moey and Whiskey whose mere existence was enough to lift my mood.

I must also thank Solar Turbines Inc and the amazing people there - Hiep Ly, Will Comenat, and Jenney Eyes - for the funding and the opportunity to pursue this project. The experience of closely collaborating with them helped drive our goals to meet realistic expectations, which is an aspect of this work I take pride on.

The material in this thesis, in part, has been submitted for publication of the material as it may appear in the Conference for Control Technology and Applications, 2024, Ramadurai, Varun; Bitmead, Robert, 2024. The thesis author was the primary researcher and author of this paper.

ABSTRACT OF THE THESIS

MIMO Process control for Compressor Systems with Recycled Flow

by

Varun Ramadurai

Master of Science in Engineering Sciences (Mechanical Engineering)

University of California San Diego, 2024

Professor Robert Bitmead, Chair

A common loop from gas processing is studied from a modeling and control perspective with an emphasis on the simplicity and control-orientation of the model components which comprise the model: pipes, branches, compressor, valves, tanks etc. The process is to take recent component model classes and to lift them to be more realistic and representative of a practical compressor operational area, notably taking into account compressor operation curves. The control objective is to improve transient response of the overall system by developing two-input controllers to manage fluctuations in either compressor suction pressure or discharge pressure in response to supply and delivery changes.

The control mechanism is the use of a recycle loop capable of transporting gas from the discharge side to the suction side – this is the faster manipulated variable – together with the slower dynamics of the compressor speed, which regulates overall flow. The return of the recycle valve to closed during steady-state operation is included into the design.

Chapter 1 Introduction

The control of gas processing facilities can be broadly split into 2 aspects: process control for operational accuracy and efficiency, and the control for safety systems that ensure the starting and stopping of operations and fast or emergency shutdowns. PID controllers have long been used for process control in the gas processing industry, with the integral action indicating the need to reject step disturbances. This classical control approach limits one to only SISO systems, requiring multiple controllers in a loop or in concentric feedback loops to stabilize more than one output variable. The manual tuning of PID gains by operators is costly and required as soon as there is a change in the plant: modifications of facility components, change of nominal operating conditions, wear of tools, etc. Further, single channel controllers assume uncoupled dynamics: each control input only affects one specific signal output which is not the case in practice.

The goal of this work is to explore modern control techniques (for their MIMO design capabilities) to replace the SISO Proportional-Integral controllers currently used. Improving the responsiveness and robustness (resilience to transient upset conditions) of the controllers would be seen as an advantage by customers that use these compressor systems for gas processing.

Kurz *et al.* [1] describe the interaction between a centrifugal compressor and the process, and as a result, the control requirements for centrifugal compressor packages with the focus on upstream and midstream applications. This work serves as the foundation to study the impact of the process behavior, and how the process dynamics impact the operation of the compressor and vice versa is analyzed, categorized, and explained. However, the scope of this thesis is limited to only the midstream, where the operations at compression stations along a pipeline are generally predictable, and the downstream, where compression equipment is used in industrial facilities to

provide regulated air and fuel gas supply to other equipment in the manufacturing process, sectors.

Brüggemann *et al.* in [2] and [3] provide the framework for the control-oriented modelling needed to develop the plant model. "Control-oriented" puts the focus of modelling on the eventual model-based feedback control reflecting the plant operational objectives, the presence and capabilities of selected actuators and sensors, and the possible reconfiguration of operations. Linear state space models are developed in [2] that describe the dynamics of pipe flows based on sets of nonlinear partial differential equations from fluid mechanics and thermodynamics together with constraints associated with their interconnection, and were validated against plant data, including the assessment of model errors.

Linearized facility-scale models were generated in [3] to describe pressures, mass flows and temperatures based on constituent equations from fluid dynamics and thermodynamics, coupled partial differential equations (PDEs) plus algebraic equations, to study a closed loop gas flow regulation problem.

The work done in this thesis is an extension of the foundation built in [2] and [3].

Contributions

Following [2], [3] and [4] which deals with developing compartmentalized component-level models for gas processing facility elements, we commence by extending this work to reflect more practically relevant and applicable approaches for valve and compressor components. The authors of [2], [3] and [4] propose simplified models for valves and compressors, which are useful in situations where the flow or compression remain constant, but

are not useful where the flow or compressor speed have to be modulated. New models for valves and compressors are developed while preserving linearity. This is particularly important in models incorporating industrial compressor operation curves, which add complexity to the models, and recycle flow valve behavior in terms of flow, which reduces complexity.

With guidance from engineers at Solar Turbines this work results in the modeling of a realistic system, analyzed from applications which involves the control of a compressor with a recycle flow valve in a loop designed to regulate pressures, which are the primary sensed variables. These systems operate in three nominal areas: upstream, midstream and downstream characterized by the nature of disturbances acting on the system. The controllability of the models were also analyzed and the models were found to require amendment and augmentation to reflect more faithfully the operating environment. The incorporation of novel model elements that better describe the dynamics of gas flows outside the domain of importance brought the system into better harmony with reality in operation.

Finally, control designs using LQG and were explored for the regulation of compressor suction and discharge pressures using compressor speed and valve flow. This suggests the utility of the control-oriented modeling approach in designing MIMO controllers.

Thesis outline

Chapter 2 reintroduces the control-oriented models of gas pipelines developed in [2] and their derivation from the basic equations of thermodynamics and fluid dynamics. This chapter works through the linearization and discretization involved in developing state space models as well as the algebraic constraints and interconnection rules required to develop composite models.

Chapter 3 deals with characterizing the problem, which includes the modelling of individual process components and their interconnected to form a networked system. New models are developed for a control valve and compressor for application where the flow rate or the compressor speed needs to be modulated. As part of the model validation, simulations are run to observe the step responses of the interconnected system to the control inputs. The interconnected model is found to lack a description of the flow dynamics upstream of the compression process and this leads to the development of a source model. Keeping in mind the eventual model-based feedback control design, anti-aliasing filters are fitted to the plant model - to move from continuous time to a sampled system - before performing model reduction to lower the order.

In Chapter 4 this reduced order model is used to develop LQG controllers to regulate the suction and discharge pressures individually. This first pass showed that the controllers did not check for the direction of flow through the valve and also kept the plant in a state of partial recycle to reject disturbances. Improvements were made to the controllers to fix these issues and it is shown how the design parameters can be adjusted to modify the controller for use in different operating conditions.

Chapter 2 Control Oriented modelling

This chapter summarizes the work done in [2] and [3] in considering the problem of control-oriented modelling for process control.

Pipe dynamics were formulated with the following assumptions:

i. The cross-sectional area of each pipe segment is constant.

ii. Average velocities across the cross section suffice for the computation of the mass flow.

iii. There is no slip at the wall, i.e., the gas velocity at the inner pipe wall is zero.

iv. Friction along the pipe can be approximated by the Darcy-Weisbach equation.

v. The compressibility factor is constant along the pipe.

vi. Capillary, magnetic, and electrical forces on the fluid are negligible.

Table 2.1 Definition of variables with units.

Symbol	Variable	Units
A	Pipe area	m
c_v	Specific heat	J/kgK
D	Pipe diameter	m
g	Gravitational acceleration	m/s^2
h	Pipe elevation	m
L	Pipe length	m
$\bar{p}$	Nominal Pressure point	Pa
p	Pressure	Pa
$\bar{q}$	Nominal mass flow point	kg/s
q	Mass flow	kg/s
q_ϕ	Rate of heat flow per unit area	W/m^2
R_s	Specific gas constant	m^2/s^2K
T	Temperature deviation from nominal point	K
T_0	Nominal temperature	K
v	Velocity	m/s
z_0	Constant compressibility factor	-
λ	Friction Factor	-
ρ	Density	kg/m^3

Under these assumptions, the constituent relations — Continuity, Momentum, Energy, Ideal Gas Equation, respectively — that serve as a basis for the models are:

$$\frac{\partial \rho}{\partial t} = -\frac{\partial (\rho v)}{\partial x} \tag{1a}$$

$$\frac{\partial (\rho v)}{\partial t} + \frac{\partial (\rho v^2 + p)}{\partial x} = -\frac{\lambda}{2D}\rho v|v| - g\rho\frac{dh}{dx} \tag{1b}$$

$$q_\rho = \frac{\partial}{\partial x}\left[\rho v\left(c_v T + \frac{v^2}{2} + gh + \frac{p}{\rho}\right)\right] + \frac{\partial}{\partial t}\left[\rho\left(c_v T + \frac{v^2}{2} + gh\right)\right] \tag{1c}$$

$$p = \rho R_s T z_0 \tag{1d}$$

2.1. Isothermal 2D model

If the assumption is also made that the temperature is constant in the length of the pipe i.e. $T(x,t) = T_0$ for all $x = [0, L]$ and $t > 0$, the Continuity, Momentum, and Ideal Gas Equations in (1) suffice to obtain :

$$\frac{\partial \rho}{\partial t} = -\frac{R_s T z_0}{A}\frac{\partial q}{\partial x} \tag{2a}$$

$$\frac{\partial q}{\partial t} = -A\frac{\partial p}{\partial x} - \frac{\lambda R_s T z_0}{2DA}\frac{q|q|}{p} - \frac{Ag}{R_s T z_0}\frac{dh}{dx}p \tag{2b}$$

Spatial discretization of (2) using simple differences results in :

$$\dot{p_r} = -\frac{R_s T z_0}{AL}(q_r - q_l) \tag{3a}$$

$$\dot{q_l} = -\frac{A}{L}(p_r - p_l) - \frac{\lambda R_s T z_0}{2DA}\frac{q_l|q_l|}{p_l} - \frac{Ag}{R_s T z_0}\frac{h}{L}p_l \tag{3b}$$

with the following boundary conditions, which are assumed to be known:

$$p_l = p(0,t), \qquad q_l = q(0,t)$$

$$p_r = p(L,t), \qquad q_r = q(L,t),$$

Subscripts $._l$ and $._r$ connote variables at left (entry) and right (exit) sides of the pipe. Input variables are identified with the pipe PDE boundary conditions, p_l, q_r and the state variables with the ODE solution, p_r, q_l.

Rearranging (3) into a state space representation we get,

$$\dot{x}_t = \begin{bmatrix} 0 & -\alpha \\ \beta & \gamma \end{bmatrix} x_t + \begin{bmatrix} 0 & \alpha \\ \kappa & 0 \end{bmatrix} u_t, \qquad y_t = x_t \tag{4}$$

with

$$\alpha = -\frac{R_S T_0 z_0}{AL}, \quad \beta = -\frac{A}{L},$$

$$\kappa = \frac{A}{L} + \frac{\lambda R_S T_0 z_0}{2DA} \frac{q_{ss}|q_{ss}|}{p_{l,ss}^2} - \frac{Agh}{R_S T_0 z_0 L},$$

$$\gamma = -\frac{\lambda R_S T_0 z_0}{DA} \frac{|q_{ss}|}{p_{l,ss}},$$

where the states and inputs are

$$x = [p_r q_l]^\top, u = [p_l \ q_r]^\top$$

2.2. Interconnection rules

To connect different pipe systems together or with other gas processing equipment, [2] lays forth the following interconnection rules:

First, we define a p-port and a q-port.

p-port of a component possesses two signals: an input pressure signal p_l and an output flow signal q_l.

q-port of a component possesses two signals: an input flow signal q_r and an output pressure signal p_r.

I. Connections are permitted only between:

   1. A p-port and a q-port, or
   2. A p-port and an external pressure source/input signal plus an external flow sink/output signal, or
   3. A q-port and an external flow source/input signal plus an external pressure sink/output signal.

II. Pressure input signals must connect to pressure output signals, and flow input signals must connect to flow output signals.

III. Connection of one variable of a port requires connection of the other.

IV. All ports must be connected, and algebraic loops avoided.

Using these rules, composite structures can now be easily defined.

2.3. Composite models

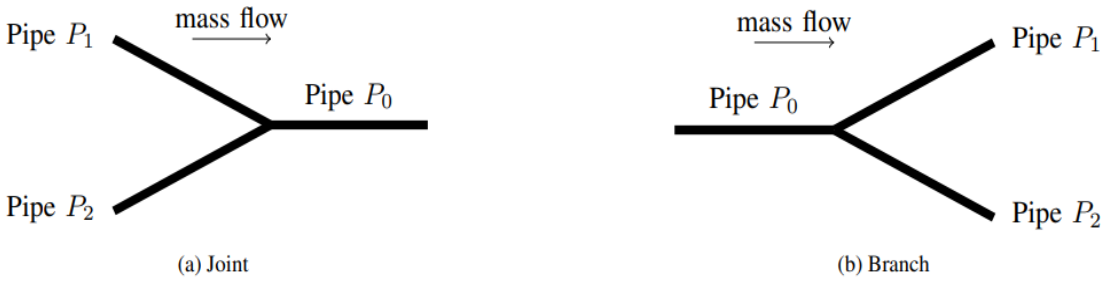

Figure 2.1 Composite pipe structures

2.3.1 Joint

Consider the joint shown in Figure 2.1a. The interconnection rules dictate the following algebraic constraints.

$$p_{0,r} = p_{1,l} = p_{2,l} \tag{5a}$$

$$q_{o,r} = q_{1,l} + q_{2,l} \tag{5b}$$

The joint model will have six states (2 for each pipe) which are:

$$[p_{0,r} \;\; p_{1,r} \;\; p_{2,r} \;\; q_{0,l} \;\; q_{1,l} \; q_{2,l}]^{\mathrm{T}}$$

But either $p_{1,r}$ or $p_{2,r}$ can be omitted due to constraint (4a) reducing the number of states to 5.

We define,

$$\delta = \frac{\alpha_1}{\alpha_1 + \alpha_2}$$

as the nominal proportion of flow for each feeding pipe.

Arbitrarily choosing to omit $p_{2,r}$, the six-state constrained system can be described as an unconstrained 5 state system:

$$\dot{x} = A_j x + B_j u, \qquad y = C_j x + D_j u \tag{6}$$

where

$$A_j = \begin{bmatrix} 0 & 0 & -\alpha_0 & 0 & 0 \\ 0 & 0 & \alpha(1-\delta) & -\alpha(1-\delta) & 0 \\ \beta_0 & \kappa_0 & \gamma_0 & 0 & 0 \\ 0 & \beta_1 & 0 & \gamma_1 & 0 \\ 0 & \beta_2 & 0 & 0 & \gamma_2 \end{bmatrix}$$

$$B_j = \begin{bmatrix} 0 & 0 & \alpha_0 \\ 0 & 0 & 0 \\ 0 & 0 & 0 \\ \kappa_1 & 0 & 0 \\ 0 & \kappa_2 & 0 \end{bmatrix}$$

$$C_j = \begin{bmatrix} 1 & 0 & 0 & 0 & 0 \\ 0 & 0 & 0 & 1 & 0 \\ 0 & 0 & 0 & 0 & 1 \end{bmatrix}$$

$$Dj = \mathbf{0_{3X3}}$$

The state, input and output vectors are now,

$$x = [p_{0,r} \;\; p_{1,r} \;\; q_{0,l} \;\; q_{1,l} \;\; q_{2,l}]^\top$$

$$u = [p_{1,l} \;\; p_{2,l} \;\; q_{0,r}\;]^\top$$

$$y = [p_{0,r} \;\; q_{1,l} \;\; q_{2,l}\;]^\top$$

2.3.2 Branch

Consider the branch shown in Figure 2.1b. The following algebraic constraints arise from the interconnection rules.

$$p_{1,r} = p_{2,r} = p_{0,l} \tag{7a}$$

$$q_{o,l} = q_{1,r} + q_{2,r} \tag{7b}$$

The pressure constraint (5a) relates the state variable, $p_{0,r}$, to input signals of the single pipe model of the branching pipes, $p_{1,l}$ and $p_{2,l}$ hence the dimension of the composite model does not reduce and the need for an additional parameter like δ is absent. The composite model retains all six states which are:

$$x = [p_{0,r} \;\; p_{1,r} \;\; p_{2,r} \;\; q_{0,l} \;\; q_{1,l} \; q_{2,l}]^\top$$

and can be described by the following linear system:

$$\dot{x} = A_b x + B_b u, \qquad y = C_b x + D_b u \tag{8}$$

where

$$A_b = \begin{bmatrix} 0 & 0 & 0 & -\alpha_0 & \alpha_0 & \alpha_0 \\ 0 & 0 & 0 & 0 & -\alpha_1 & 0 \\ 0 & 0 & 0 & 0 & 0 & -\alpha_2 \\ \beta_0 & 0 & 0 & \gamma_0 & 0 & 0 \\ \kappa_1 & \beta_1 & 0 & 0 & \gamma_1 & 0 \\ \kappa_2 & 0 & \beta_2 & 0 & 0 & \gamma_2 \end{bmatrix}$$

$$B_b = \begin{bmatrix} 0 & 0 & 0 \\ 0 & \alpha_1 & 0 \\ 0 & 0 & \alpha_2 \\ \kappa_0 & 0 & 0 \\ 0 & 0 & 0 \\ 0 & 0 & 0 \end{bmatrix}$$

$$C_b = \begin{bmatrix} 0 & 1 & 0 & 0 & 0 & 0 \\ 0 & 0 & 1 & 0 & 0 & 0 \\ 0 & 0 & 0 & 1 & 0 & 0 \end{bmatrix}$$

$$D_b = \mathbf{0_{3X3}}$$

The input and output vectors are:

$$u = [p_{0,l} \;\; q_{1,r} \;\; q_{2,r}\;]^{\top}$$

$$y = [p_{1r} \;\; p_{2,l} \;\; q_{0,l}\;]^{\top}$$

Chapter 3 Problem development

The process flow diagram below in Figure 1.2 is a typical arrangement for a gas compression application. The driver is a gas turbine engine or electric motor (EMD) that drives a centrifugal gas compressor (CP-100). Process gas enters through the suction valve (SV-100) and into the compressor. The gas is heated as a result of the compression process and typically goes into an air-gas heat exchanger (C-100). The process gas exits the system through a check valve and a discharge valve (DV-100).

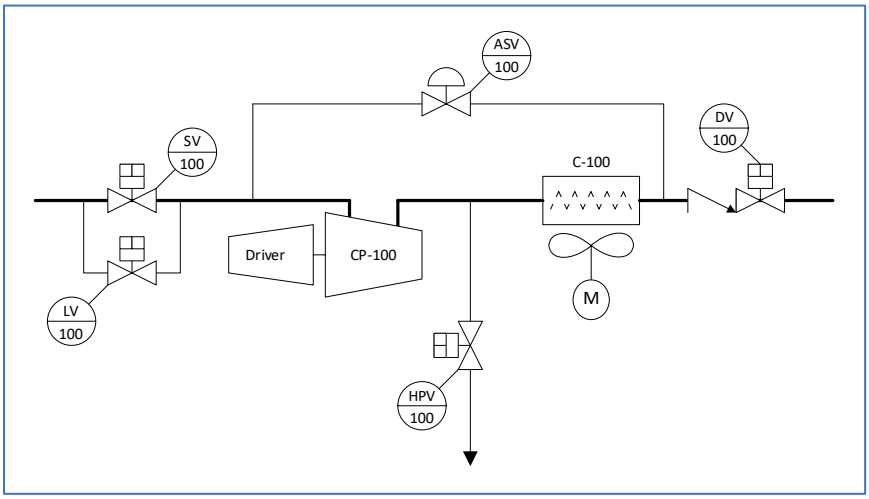

Figure 3.1 Example Process Flow Diagram

The power delivered to the compressor is regulated to control the compressor speed and therefore the compressor flow and system pressures. In some cases, it is necessary to recycle an amount of process gas from compressor discharge to suction through ASV-100, which is a valve that can be regulated by the control system. This allows extended periods of recycle while keeping the process gas temperature below its upper limit (shutdown setpoint). The vent valve (HPV-100) is used to vent process gas to bring the piping and compressor to or near ambient pressure when not in operation. To stop the system, the driver power is shut off and the driver

and compressor coast to a near stop before the vent valve is opened. The loading valve (LV-100) is used to purge oxygen and pressurize the system when starting from a ventilated state. It is usually a 1" to 3" valve that allows high pressure gas into the system at a gradual rate.

Compared to Figure 3.1, the process flow diagram is simplified in Figure 3.2 and is the basis for the control oriented modelling. The simplified version only includes six pipes, the ASV, the compressor and the EMD. The heat exchanger, the suction and discharge valves, and the low & high pressure valves were not included as they are not critical to understanding the process dynamics. The pipe system (P1, P2, P3), pipe system (P4, P6, P6), the valve, and the compressor (with the EMD) are each modelled separately and connected together.

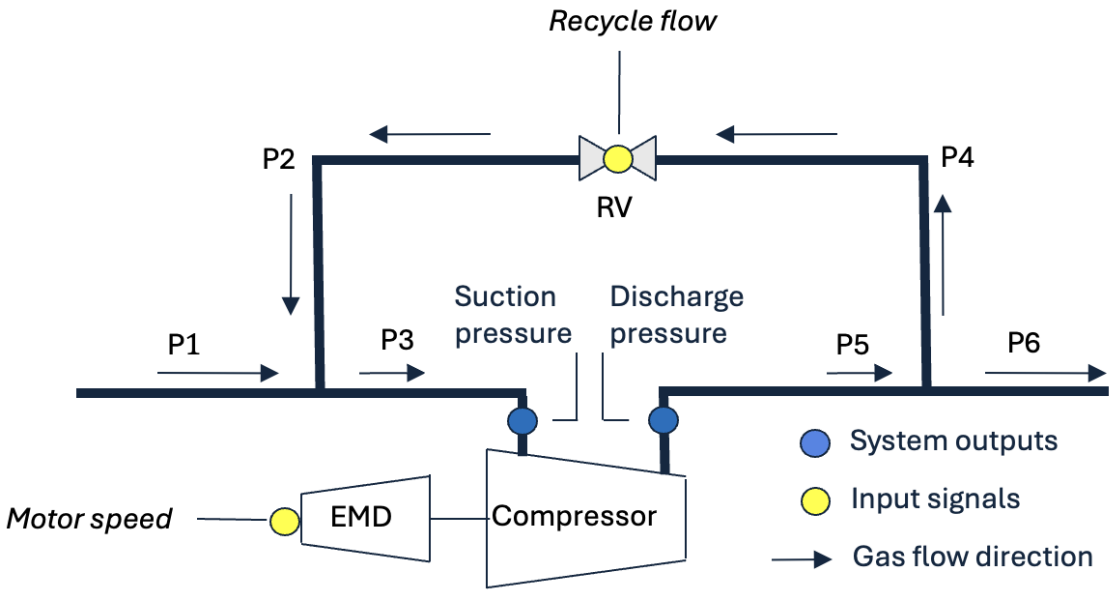

Figure 3.2 Simplified process flow diagram for model construction. Compressor speed command signal and valve flow command (yellow circles); and outputs, suction pressure and discharge pressure (blue circles).

3.1. Compressor and EMD models

The EMD is modelled as a first-order lag having the following transfer function:

$$\frac{\tau}{s+\tau}$$

with the input being the desired compressor speed w_τ and the output being the delayed command to the compressor w. A time constant of $\tau = 2$ is representative, resulting in the following model:

$$w_\tau = \frac{2}{s+2}\, w \tag{9}$$

The transfer function model in (9) can be expressed in the following state space form:

$$\dot{x} = A_m x + B_m u, \quad y = C_{mx} + D_m u \tag{10}$$

with $A_m = -2,\ B_m = 1,\ C_m = 2,\ D_m = 0.$

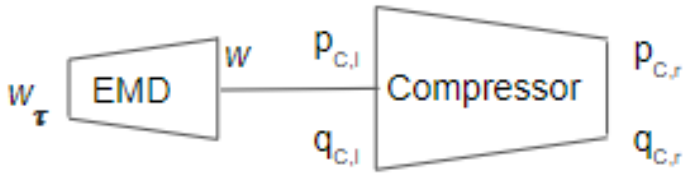

Figure 3.3 Compressor + EMD system

Brüggemann *et al.* [3] proposes two models for a compressor. The first uses a static gain (greater than 1) on pressure and a unity gain on mass flow,

$$x = \begin{bmatrix} k\_c & 0 \\ 0 & 1 \end{bmatrix} u \tag{11}$$

where $k_c > 1$ and,

$$x = [p_{c,r},\ q_{c,l}]^\top, \quad u = [p_{c,l},\ q_{c,r}]^\top$$

and the second uses a static compressor map:

$$p_{c,r} = \phi(w,\ p_{c,l},\ q_{c,r}) \tag{12}$$

that describes the discharge pressure as a function of suction pressure, compressor speed and mass flow rate through the compressor, connected to a duct and a plenum. Since

the first model (11) does not use compressor speed as an input, a version of the second model (12) that only uses the static map (without the added duct and plenum for simplicity) is used to model the compressor.

This static map is derived by linearization of the compressor's performance curves (provided by Solar Turbines).

The following assumptions are made:

i. Compression is isentropic.

ii. Friction in the compressor is negligible.

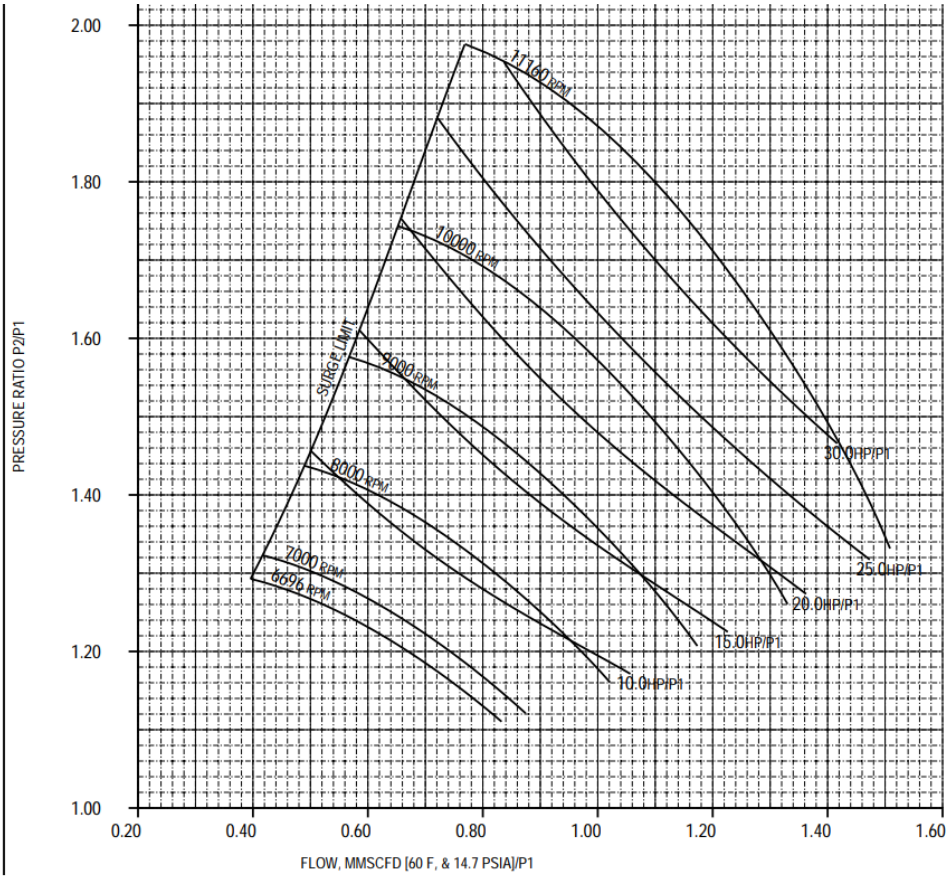

Figure 3.4 Compressor performance curves.

The compressor performance chart in Figure 3.2 is linearized about the point at 1 million standard cubic feet per day (MMSCFD) per unit of suction pressure (1 MMSCFD = 0.25 kg/s) and 10000 rpm to produce the following linear equation:

$$p_{c,r} = 1{,}57p_{c,l} + 890.02w_{\tau} - 1.7237 * 10^{5}q_{c,r} \quad (13)$$

Where $p_{c,r}$ is the pressure at the right end of the compressor (discharge pressure), $p_{c,l}$ is the pressure at the left end of the compressor (suction pressure), $q_{c,r}$ is the flow rate at the right end of the compressor and w is the delayed compressor speed from the EMD.

Since flow through the compressor is conserved,

$$q_{c,l} = q_{c,r} \quad (14)$$

(13) and (14) can be combined and the compressor can modeled in a state space representation where the states, inputs and outputs are:

$$x = \begin{bmatrix} p_{c,r} & q_{c,l} \end{bmatrix}^{\top}, u = \begin{bmatrix} w & p_{c,l} & q_{c,r} \end{bmatrix}^{\top}, y = \begin{bmatrix} p_{c,r} & q_{c,l} \end{bmatrix}^{\top}$$

with the relationship be defined as,

$$\dot{x} = A_c x + B_c u, \quad y = C_c x + D_c u \quad (15)$$

where,

$$A_c = 0, B_c = 0, C_c = 0, D_c = \begin{bmatrix} 890.02 & 1.57 & -1.7237e^{5} \\ 0 & 0 & 1 \end{bmatrix}$$

3.2. Valve model

Brüggemann *et al.* [3] also proposes two models for a control valve. Similar to the compressor, the first model uses a static gain (less than or equal to 1) on the pressure and a unity gain on the mass flow,

$$x = \begin{bmatrix} k_v & 0 \\ 0 & 1 \end{bmatrix} u \quad (16)$$

where $k_v < 1$ and,

$$x = [p_{v,r},\ \ q_{v,l}]^{\mathbb{T}},\quad u = [p_{v,l},\ \ q_{v,r}]^{\mathbb{T}}$$

And the second is a dynamic model based on the static relationship used for orifices combined with a first order low pass filter to approximate the dynamics between command and actuation.

$$\dot{x} = [-1/\tau]x + [K/\tau\ \ 0\ \ 0]u \tag{17a}$$

$$y = [g_0(A_0, \bar{p}_l, \bar{p}_r)/A_0]x + [0\ \ \zeta_0(A_0, \bar{p}_l, \bar{p}_r)\ \ \xi_0(A_0, \bar{p}_l, \bar{p}_r)]u \tag{17b}$$

where,

$$x = [A_0],\ \ y = [q_v],\quad u = [u_v\ \ p_{v,l}\ \ p_{v,r}]$$

and

$$g_0(A_0, \bar{p}_l, \bar{p}_r) = q_0 = Cp_{0,l}A_0\sqrt{\frac{2}{R_s T z_0}\frac{\mu}{\mu-1}\left[\left(\frac{p_{0,r}}{p_{0,l}}\right)^{2/\mu} - \left(\frac{p_{0,r}}{p_{0,l}}\right)^{\mu+1/\mu}\right]} \tag{18}$$

$$\xi_0(A_0, \bar{p}_l, \bar{p}_r) = \frac{\partial g_0(A_0, \bar{p}_l, \bar{p}_r)}{\partial p_r} \tag{19a}$$

$$\zeta_0(A_0, \bar{p}_l, \bar{p}_r) = \frac{\partial g_0(A_0, \bar{p}_l, \bar{p}_r)}{\partial p_l} \tag{19b}$$

$$A_0 = K\frac{\tau}{\tau s+1}u_v \tag{20}$$

g_0 is the orifice equation from (18), τ and K the time constant and gain from transfer function (20) between the control command and actual actuation, $q_v$the mass flow through the valve, $u_v \in (0,\ 1)$ the control input, A_0 the cross-sectional area of the valve, and ξ_0 and ζ_0 the linearization terms from (19a) and (19b)

The first model (16) is useful in situations where the valve is to be modelled at a fixed opening but does not allow for modulation of the flow rate through the valve making it

unsuitable in cases (like ours) where the flow rate through the valve is to be an input. The second model (17) is a linear approximation of a nonlinear relationship making it complicated to model and prone to errors at operating points away from the point of linearization.

Thus, a new model is developed that allows the flow rate through the valve to be directly controlled instead of setting a valve opening or pressure gain.

Let the sates, inputs and outputs be,

$$x = \begin{bmatrix} q_{v,l} & q_{v,r} \end{bmatrix}^{\top}, u = [q_u], y = \begin{bmatrix} q_{v,l} & q_{v,r} \end{bmatrix}^{\top}$$

where $q_{v,l}$ and $q_{v,r}$ are the mass flows at the left and right ends of the valve respectively and q_u is the commanded flow through the valve, and the relationship be defined as,

$$\dot{x} = A_v x + B_v u, y = C_v x + D_v u \quad (21)$$

where,

$$A_v = 0, B_v = 0, C_v = 0, D_v = \begin{bmatrix} -1 \\ 1 \end{bmatrix}$$

This reimagining of the model removes the need to consider the physical nonlinearity of the valve, keeping the model linear without any approximation errors due to linearization. In terms of the process, the valve is simply an input signal that removes and adds flow from its inlet and discharge sides respectively. Conservation of mass is immediate.

3.3. Pipe Systems

From figure 3.1 it can be seen that the mass flows from pipes 1 and 2 join into pipe 3. If this system is modelled as a joint (5) the inputs and outputs would be

$$u = [p_{1,l} \quad p_{2,l} \quad q_{0,r}]^{\top}$$

$$y = [p_{0,r} \quad q_{1,l} \quad q_{2,l}]^{\top}$$

Since the left end of pipe 2 is described by a q-port (because of the signals $p_{2,l}$ and $q_{2,l}$) and the outputs of the valve model ($q_{v,l}$ and $q_{v,r}$) are also q-ports, the valve cannot be connected to the left end of pipe 2 because connections are only permitted between p-ports and q-ports.

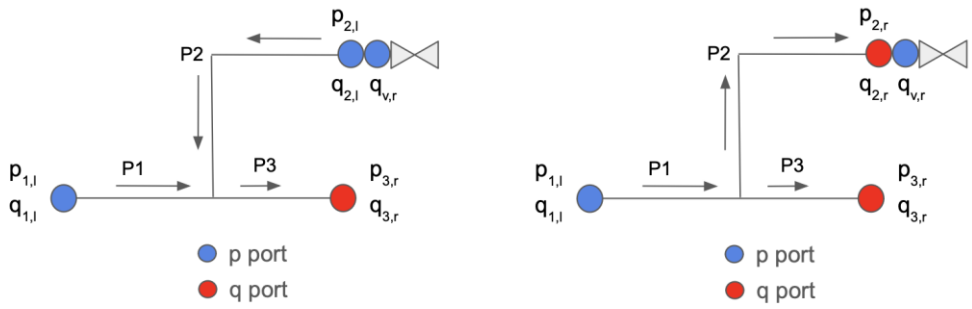

(a) (b)

Figure 3.5 (a) Valve and pipe 2 connection if modelled as a joint. (b) Valve and pipe 2 connection if modeled as a branch

Hence, the system of pipes P1, P2 & P3 is reimagined as a branch with negative flow (flow direction is right to left instead of conventional left to right) through pipe 2. There is now a q-port input ($q_{2,r}$) that can be connected to the q-port of the valve output ($q_{v,l}$) to satisfy the interconnection rules as seen in Figure 3.4 (b).

This leads to the following state space model:

$$\dot{x} = A_{jb}x + B_{jb}u, \qquad y = C_{jb}x + D_{jb}u \tag{22}$$

where,

$$A_{jb} = \begin{bmatrix} 0 & 0 & 0 & -\alpha_1 & \alpha_1 & \alpha_1 \\ 0 & 0 & 0 & 0 & -\alpha_2 & 0 \\ 0 & 0 & 0 & 0 & 0 & -\alpha_3 \\ \beta_1 & 0 & 0 & \gamma_1 & 0 & 0 \\ \kappa_2 & \beta_2 & 0 & 0 & \gamma_2 & 0 \\ \kappa_3 & 0 & \beta_3 & 0 & 0 & \gamma_3 \end{bmatrix}$$

$$B_{jb} = \begin{bmatrix} 0 & 0 & 0 \\ 0 & \alpha_2 & 0 \\ 0 & 0 & \alpha_3 \\ \kappa_1 & 0 & 0 \\ 0 & 0 & 0 \\ 0 & 0 & 0 \end{bmatrix}$$

$$C_{jb} = \begin{bmatrix} 0 & 1 & 0 & 0 & 0 & 0 \\ 0 & 0 & 1 & 0 & 0 & 0 \\ 0 & 0 & 0 & 1 & 0 & 0 \end{bmatrix}$$

$$D_{jb} = \mathbf{0_{3X3}}$$

$\alpha, \beta, \gamma \; and \; \kappa$ are the constants defined in (4).

The states, inputs and outputs are:

$x = [p_{1,r} \;\; p_{2,r} \;\; p_{3,r} \;\; q_{1,l} \;\; q_{2,l} \;\; q_{3,l}]^{\top}$, $u = [p_{1,l} \;\; q_{2,r} \;\; q_{3,r}]^{\top}$, $y = [p_{2,r} \;\; p_{3,r} \;\; q_{1,l}]^{\top}$

The flow from pipe 5 branches out into pipes 4 and 6 as seen in Figure 3.1 so the system of pipes 4, 5 & 6 is modelled as a branch (7a) & (7b) with the following state space model:

$$\dot{x} = A_b x + B_b u, \quad y = C_b x + D_b u \tag{23}$$

where

$$A_b = \begin{bmatrix} 0 & 0 & 0 & -\alpha_5 & \alpha_5 & \alpha_5 \\ 0 & 0 & 0 & 0 & -\alpha_4 & 0 \\ 0 & 0 & 0 & 0 & 0 & -\alpha_6 \\ \beta_5 & 0 & 0 & \gamma_5 & 0 & 0 \\ \kappa_6 & \beta_4 & 0 & 0 & \gamma_4 & 0 \\ \kappa_3 & 0 & \beta_6 & 0 & 0 & \gamma_6 \end{bmatrix}$$

$$B_b = \begin{bmatrix} 0 & 0 & 0 \\ 0 & \alpha_4 & 0 \\ 0 & 0 & \alpha_6 \\ \kappa_5 & 0 & 0 \\ 0 & 0 & 0 \\ 0 & 0 & 0 \end{bmatrix}$$

$$C_b = \begin{bmatrix} 0 & 1 & 0 & 0 & 0 & 0 \\ 0 & 0 & 1 & 0 & 0 & 0 \\ 0 & 0 & 0 & 1 & 0 & 0 \end{bmatrix}$$

$$D_b = \mathbf{0_{3X3}}$$

And the following states, inputs and outputs:

$$x = \begin{bmatrix} p_{5,r} & p_{4,r} & p_{6,r} & q_{5,l} & q_{4,l} & q_{6,l} \end{bmatrix}^{\top}, u = \begin{bmatrix} p_{5,l} & q_{4,r} & q_{6,r} \end{bmatrix}^{\top}, y = \begin{bmatrix} p_{4,r} & p_{6,r} & q_{5,l} \end{bmatrix}^{\top}$$

3.4. Interconnected system

Brüggemann *et al.* in [1] introduced a matrix formulation that enables the construction of state-space models for N interconnected components:

$$\dot{x} = Ax + Bw, \; y = Cx + Dw \tag{24a}$$

$$w = Fy + Gu \tag{24b}$$

where,

$$A = blkdiag(A^{(1)}, A^{(2)}, \ldots . A^{(N)})$$

$$B = blkdiag\left(B^{(1)}, B^{(2)}, \ldots . B^{(N)}\right)$$

$$C = blkdiag\left(C^{(1)}, C^{(2)}, \ldots . C^{(N)}\right)$$

$$D = blkdiag(D^{(1)}, D^{(2)}, \ldots . D^{(N)})$$

$$F_{i,j} = \begin{cases} 1, & if\ y_j = w_i \\ 0, & if\ otherwise \end{cases}$$

$$G_{i,j} = \begin{cases} 1, & if\ u_j = w_i \\ 0, & if\ otherwise \end{cases}$$

x is the total state vector,

u is the total input vector to the system,

y is the total output vector ,

w is the component input vector.

Applying this matrix methodology to the system in Figure 3.1 results in the following model:

$$\dot{x} = A_t x + B_t w,\ y = C_t x + D_t w \tag{25}$$

where,

$$A = blkdiag(A_{jb}, A_b, A_c, A_v, A_m)$$

$$B = blkdiag(B_{jb}, B_b, B_c, B_v, B_m)$$

$$C = blkdiag(C_{jb}, C_b, C_c, C_v, c_m)$$

$$D = blkdiag(D_{jb}, D_b, D_c, D_v, D_m)$$

And the following vectors:

$x = [p_{1,r}\ \ p_{2,r}\ \ p_{3,r}\ \ q_{1,l}\ \ q_{2,l}\ \ q_{3,l}\ \ p_{4,r}\ \ p_{5,r}\ \ p_{6,r}\ \ q_{4,l}\ \ q_{5,l}\ \ q_{6,l}\ \ q_{v,r}\ \ q_{v,l}\ \ p_{c,r}\ \ q_{c,l}\ \ w\ ]^{\top}$,

$u = [w_{\tau}\ \ q_u\ \ p_{1,l}\ \ q_{6,r}]^{\top}$,

$y = [p_{2,r}\ \ p_{3,r}\ \ q_{1,l}\ \ p_{4,r}\ \ p_{6,r}\ \ q_{5,l}\ \ p_{c,r}\ \ q_{c,l}\ \ q_{v,r}\ \ q_{v,l}\ \ w]^{\top}$,

$w = [\ p_{1,l}\ \ q_{2,r}\ \ q_{3,r}\ \ p_{4,r}\ \ p_{5,l}\ \ q_{4,r}\ \ q_{6,r}\ \ q_{v,l}\ \ q_{v,r}\ \ p_{c,l}\ \ q_{c,r}\ ]^{\top}$.

The boundary conditions are:

$$p_{3,r} = p_{c,l},\quad p_{5,l} = p_{c,r},\quad p_{2,r} = p_{v,r},\quad p_{4,r} = p_{v,l}$$

$$q_{3,r} = q_{c,l},\quad q_{5,l} = q_{c,r},\quad q_{2,r} = q_{v,r},\quad q_{4,r} = q_{v,l}$$

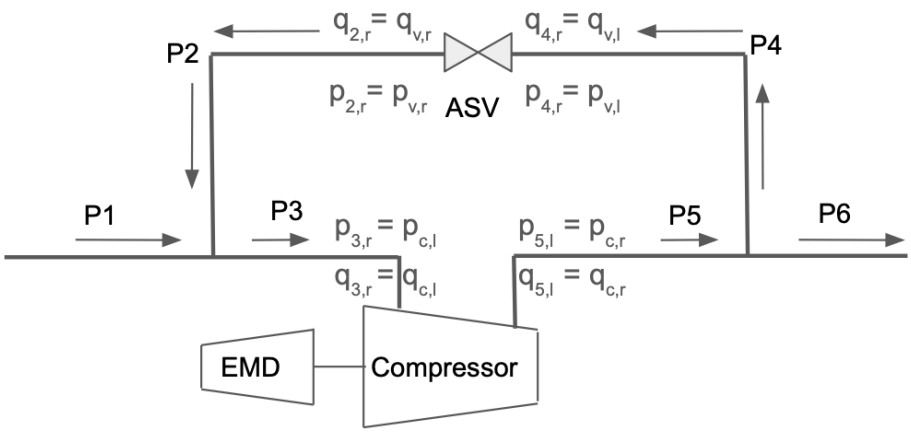

Figure 3.6 Diagram showing boundary conditions.

An alternative to the above matrix methodology is MATLAB™'s 'connect' function[1]. For each component in the networked system, the input and output signals are defined while respecting boundary conditions, the input and desired output signals of the interconnected system are also defined and the 'connect' function is called.

[1] See appendix A for MATLAB™ definitions and interconnected system construction.

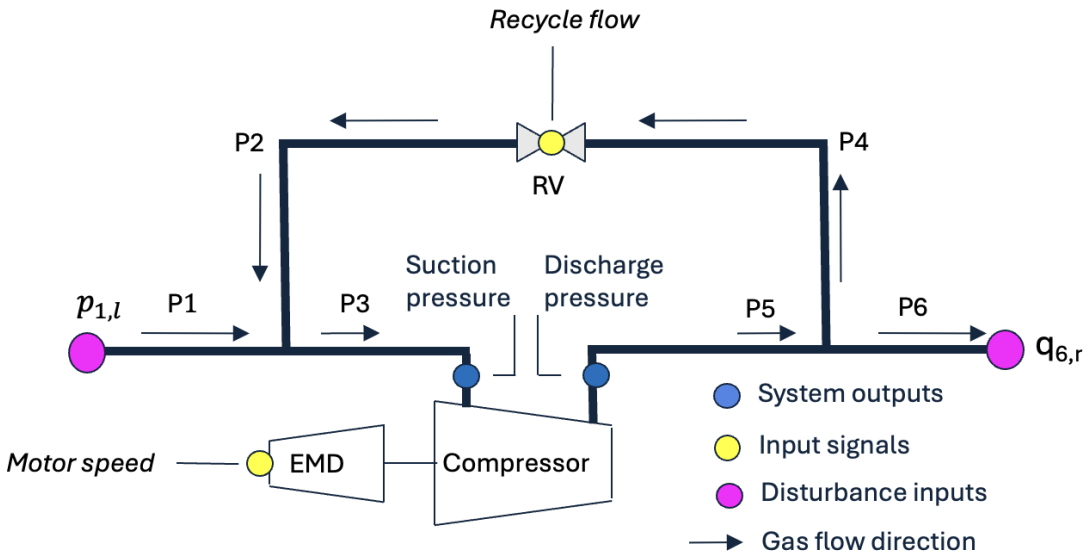

Figure 3.7 Schematic diagram of the compressor recycle loop with: inputs, compressor speed command signal and valve flow command (yellow circles); disturbance inputs, upstream pressure and downstream flow (pink circles); and, outputs, suction pressure and discharge pressure (blue circles).

The interconnected system has 4 inputs. $u = \begin{bmatrix} w_\tau & q_u & p_{1,l} & q_{6,r} \end{bmatrix}^\top$. w_τ and q_u are the two control inputs (compressor speed command and the valve flow command). $p_{1,l}$ and $q_{6,r}$ are extrernal inputs to the system , as these are the component inputs to pipe system P1, P2, P3 and P4, P5, P6 respectively that are not connected to any other ports.

Since both the compressor and valve are modelled as a direct feedthrough (Output at the current timestep depends only the input at the current timestep. No system dynamics.), the zero-direct-feedthrough (D=0) property of the EMD model (10) prevents the appearance of an algebraic loop between the inputs and outputs of the compressor and valve from forming in such a closed loop system.

3.5. Source model

The external inputs to the system $p_{1,l}$ and $q_{6,r}$ play a crucial role in the behavior of the system. $q_{6,r}$, which describes the flow at the right end of P6 is constant with respect to the system since it is external input. As a result, the total flow in the interconnected system is conserved and no flow extra flow can enter or leave the system without having to change the input $q_{6,r}$.

Secondly, the suction pressure ($p_{3,r}$) is a function of the inlet pressure ($p_{1,l}$) as described by (22). Since the inlet pressure is the only input to the joint system of P1,P2,P3 and is constant with respect to the interconnected system, the suction pressure is also forced to be constant. To make the inlet pressure a state of the system, the dynamics of the flow before the inlet to the system needs to be described. This fact motivates the need for a model describing the source of the gas flow.

The source of natural gas into the compressor system is modelled as pipes attached to the isothermal tank model developed in [3].

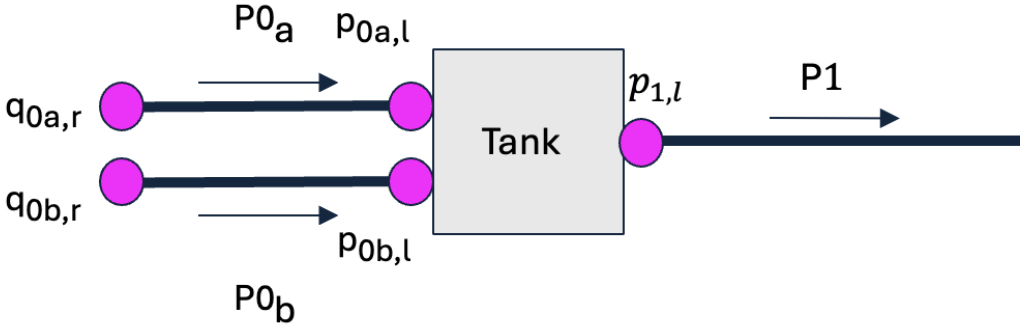

Figure 3.8 Example of source with 2 wells

The tank has a single state that describes the pressure inside the tank volume $x = p_t$ and inputs $u = \{q_{1,i} \ldots\ldots q_{n_i,i} \quad q_{1,o} \ldots\ldots q_{n_o,o}\}^T$ where n_i and n_0 are the number of inlet and outlet pipes respectively and :is described by the relationship:

$$\dot{x} = \frac{R_s z_0 T_0}{V} [1_{n,i} \quad -1_{n,o}] \tag{26}$$

The inlet pressure ($p_{1,l}$) is now the same as the tank pressure (p_t). This allows the inlet pressure to change as a function of other system states instead of being an external input to the interconnected system. Having the inlet pressure as a system state consequently allows the suction pressure ($p_{3,r}$) to change with compressor speed and recycled flow.

Each pipe attached to the tank represents a natural gas well, and the length and diameter of the pipe are chosen to mimic properties of the well such as density and porosity of the rocks.

Arbitrarily choosing to model two wells as two pipes $P_{0,a}$ and $P_{0,b}$:

$$\dot{x} = A_{0,a}x + B_{0,a}u, \qquad y = x \tag{27}$$

$$\dot{x} = A_{0,b}x + B_{0,b}u, \qquad y = x \tag{28}$$

where

$$A_{0,a} = \begin{bmatrix} 0 & -\alpha_{0,a} \\ \beta_{0,a} & \gamma_{0,a} \end{bmatrix}, B_{0,b} = \begin{bmatrix} 0 & \alpha_{0,a} \\ \kappa_{0,a} & 0 \end{bmatrix}$$

$$A_{0,b} = A_{0,a},\ B_{0,b} = B_{0,a}$$

the states and inputs are

$x = [p_{0a,r} \ \ q_{0a,l}]^\top$, $u = [p_{0a,l} \ \ q_{0a,r}]^\top$ for pipe $P_{0,a}$

$x = [p_{0b,r} \ \ q_{0b,l}]^\top$, $u = [p_{0b,l} \ \ q_{0b,r}]^\top$ for pipe $P_{0,b}$

$\alpha, \beta, \gamma \ and \ \kappa$ are the constants defined in (4).

The source model is then the connection of the two pipes and the tank, described by the following relationship:

$$\dot{x} = A_s x + B_s u, \quad y = C_s x + D_s u \tag{29}$$

where

$$A_s = \begin{bmatrix} 0 & -\alpha_{0a} & 0 & 0 & 0 & 0 \\ 0 & \gamma_{0a} & 0 & 0 & 0 & 0 \\ \beta_{0a} & 0 & 0 & -\alpha_{0b} & 0 & 0 \\ 0 & 0 & \beta_{0b} & \gamma_{0b} & 0 & 0 \\ 0 & 0 & 0 & 0 & 0 & 0 \\ 0 & \frac{R_s z_0 T_0}{V} & 0 & \frac{R_s z_0 T_0}{V} & 0 & 0 \end{bmatrix}$$

$$B_s = \begin{bmatrix} 0 & \alpha_{0a} & 0 & 0 & 0 & 0 \\ \kappa_{0a} & 0 & 0 & 0 & 0 & 0 \\ 0 & 0 & \kappa_{0b} & \alpha_{0b} & 0 & 0 \\ 0 & 0 & 0 & 0 & 0 & 0 \\ 0 & 0 & 0 & 0 & 0 & 0 \\ 0 & 0 & 0 & 0 & 0 & \frac{-R_s z_0 T_0}{V} \end{bmatrix}$$

$$C_S = I_5$$

$$D_s = 0_5$$

And has the following states inputs and outputs:

$$x = [p_{0a,r} \quad q_{0a,l} \quad p_{0b,r} \quad q_{0b,l} \quad p_t]^\top$$

$$u = [p_{0a,l} \quad q_{0a,r} \quad p_{0b,l} \quad q_{0b,r} \quad q_{1,o}]^\top$$

$$y = [p_{0a,r} \quad q_{0a,l} \quad p_{0b,r} \quad q_{0b,l} \quad p_t]^\top$$

Modelling the source in this way also allows the same model to be used for midstream and upstream applications (described in Chapter 1) by changing the tank size. Having a tank with an extremely large volume (order of 10^9 m^3) would result in the tank pressure being almost constant since the change in tank pressure is inversely proportional to tank volume (see (13)) , resulting in constant suction pressure. This mimics the midstream application of gas compressors

where the pipelines are packed to a constant pressure, thus changing the compressor speed or mass flow rate through the ASV does not affect the suction pressure.

It is important to note here that just as a description of the dynamics upstream of the interconnected system was crucial to eliminate the effects of having a constant inlet pressure ($p_{1,l}$), a description of the dynamics downstream of the interconnected system will also remove any effects the forced conservation of flow through the system due to the outlet flow ($q_{6,r}$) being held constant. However, no such description is derived because the effects of the conservation do not affect the control problem being addressed, which is the regulation of suction and discharge pressure.

3.6. Interconnected system with source model

Figure 3.6 shows the complete interconnected system. There are 5 disturbances in total. Two pressure and two flow disturbances upstream, and one flow disturbance downstream of the compressor system.

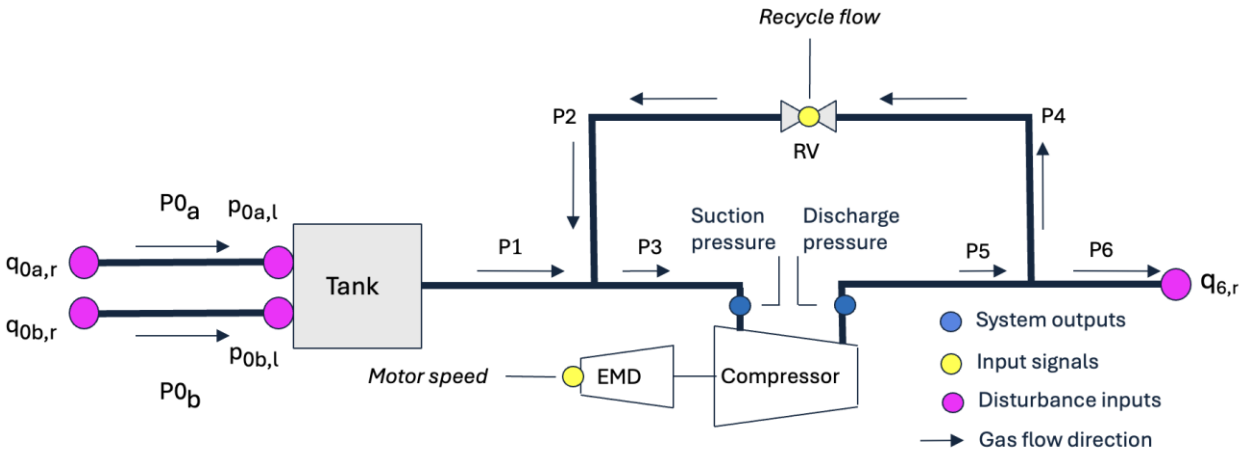

Figure 3.9 Interconnected system with source model showing the inputs, compressor speed command signal and valve flow command (yellow circles); disturbance inputs, upstream pressure and downstream flow (pink circles); and, outputs, suction pressure and discharge pressure (blue circles).

The interconnected system along with the source model describes both the input to output relationship (plant model) as well as the disturbance to output relationship (disturbance model).

Connecting the source model (27) to the interconnected system (25a) & (25b) results in the following system[2]:

[2] See appendix A for MATLAB code using connect function

$$\dot{x} = Ax + Bw,\ y = Cx + Dw \quad (30)$$

where,

$$A = blkdiag(A_t, A_s)$$

$$B = blkdiag(B_t, B_s)$$

$$C = blkdiag(C_t, C_s)$$

$$D = blkdiag(D_t, D_s)$$

with the added boundary condition $p_t = p_{1,l} = p_{0a,l} = p_{0b,l}$

And the following vectors:

$x = [\ p_{1,r}\ p_{2,r}\ p_{3,r}\ q_{1,l}\ q_{2,l}\ q_{3,l}\ p_{4,r}\ p_{5,r}\ p_{6,r}\ q_{4,l}\ q_{5,l}\ q_{6,l}$

$q_{2,r}\ q_{4,r}\ p_{5,l}\ q_{3,r}\ w\ q_{0a,l}\ p_{0a,r}\ q_{0b,l}\ p_{0b,r}\ p_{1,l}]^{\top}$

$u = [w_\tau\ \ q_u\ \ p_{0a,l}\ \ q_{0a,r}\ \ p_{0b,l}\ \ q_{0b,r}\ \ q_{6,r}]^{\top}$,

$y = [p_{2,r}\ \ p_{3,r}\ \ q_{1,l}\ \ p_{4,r}\ \ p_{6,r}\ \ q_{5,l}\ \ p_{c,r}\ q_{c,l}\ q_{v,r}\ q_{v,l}\ w\ p_{1,l}\ p_{0a,r}\ \ q_{0a,l}\ \ p_{0a,r}\ \ q_{0a,l}]^{\top}$,

$w = [\ p_{1,l}\ \ q_{2,r}\ \ q_{3,r}\ \ p_{4,r}\ \ p_{5,l}\ \ q_{4,r}\ \ q_{6,r}\ \ q_{v,l}\ \ q_{v,r}\ \ p_{c,l}\ \ q_{c,r}\ \ p_{0a,l}\ q_{0a,r}\ p_{0b,l}\ \ q_{0b,r}]^{\top}$.

The plant and disturbance dynamics are described together by the interconnected system and the resulting model is a 22nd order system.

The commanded compressor speed (w_τ) and ASV flow (q_u) are the two control signals used to regulate the suction and discharge pressure, and the other five inputs ($q_{6,r}$, $q_{0a,r}$, $p_{0a,l}$, $q_{0b,r}$, $p_{0b,l}$) represent the sources of disturbances : downstream flow arising from fluctuations in gas demand, and upstream pressures and flows arising from fluctuations in the wells.

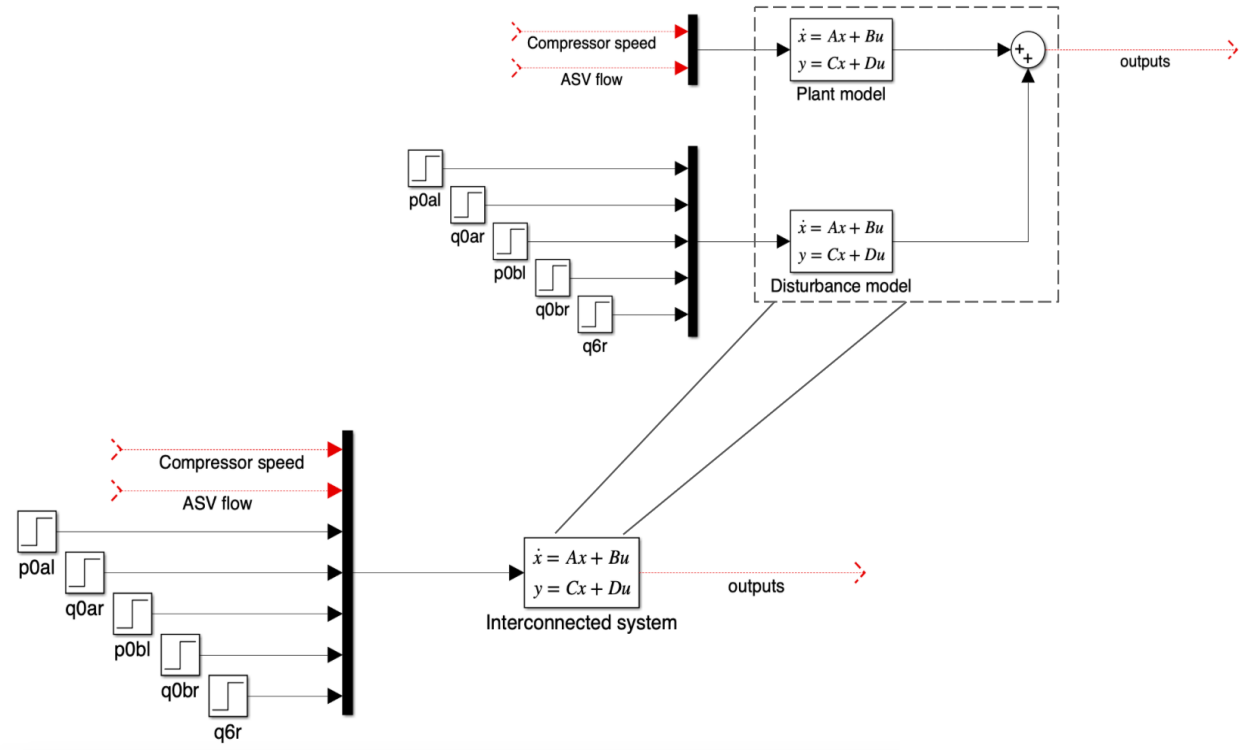

Figure 3.10 Interconnected system consisting of plant and disturbance model.

3.7. Model behavior

3.7.1 Step responses

To test the validity of the model, step changes were applied to each control input (compressor speed and ASV flow) individually to see if the response of the outputs (suction and discharge pressures) matched with predicted behavior. We expect to see the suction pressure increase and the discharge pressure decrease for a decrease in compressor speed, or for an increase in the ASV flow.

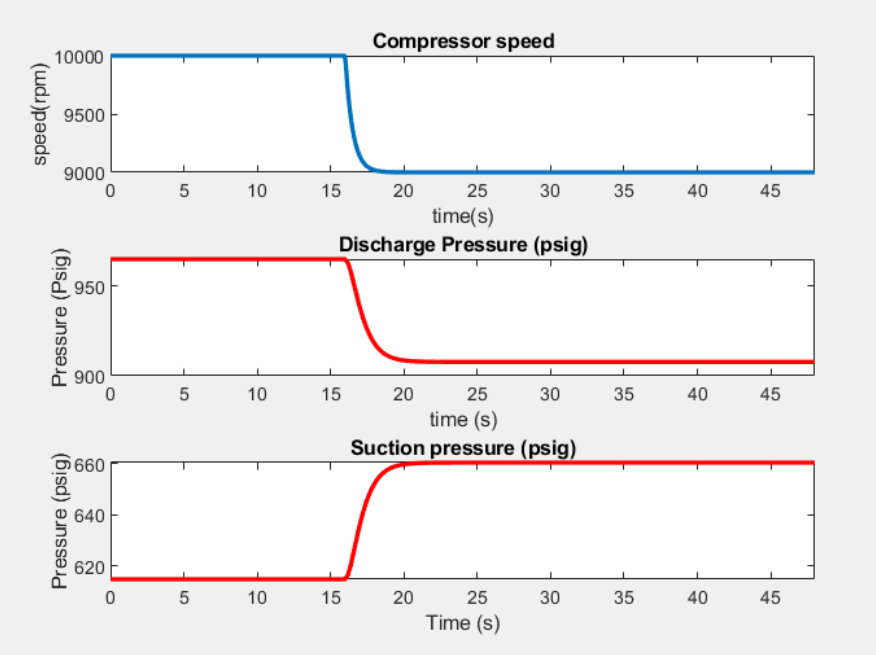

Figure 3.11 Step responses to compressor speed

Figure 3.7 shows the results of stepping down the compressor speed.

- The compressor speed input shows a lag because of the motor drive.
- The compressor performance curves (Figure 3.3) show that decrease in compressor speed results in a decrease in the discharge to suction pressure ratio for a constant mass flow rate through the compressor.
- This causes the discharge pressure to decrease and the suction pressure to increase.

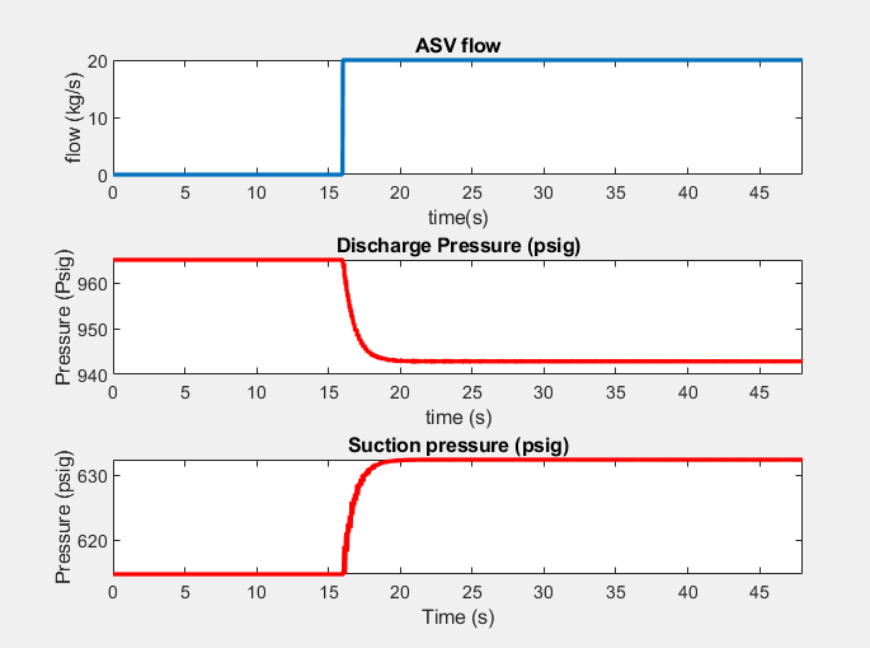

Figure 3.12 Step responses to ASV flow

A similar effect is observed when the compressor speed is kept constant and mass flow rate through the ASV is increased.

- When flow is recycled through the ASV, the flow rate at the discharge end of the compressor is reduced, causing the discharge pressure to drop.
- The flow rate at the suction side of the compressor is increased due to the extra flow from the ASV, causing the suction pressure to rise.

Step changes to the inputs were also applied to the interconnected system with an extremely large tank volume (10^9 m^3) to simulate a constant suction pressure condition since the change in suction pressure is inversely proportional to tank volume (see (13)).

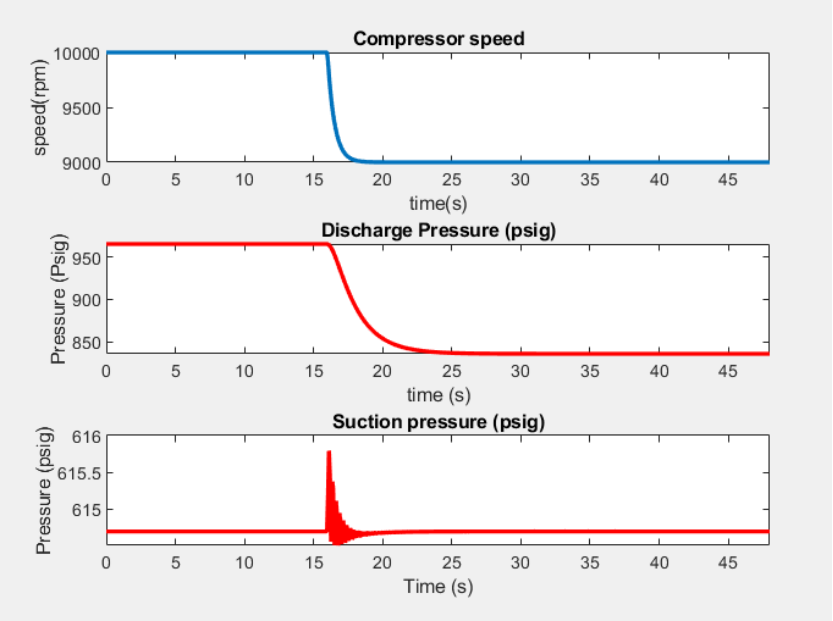

Figure 3.13 Step responses to compressor speed for packed midstream application

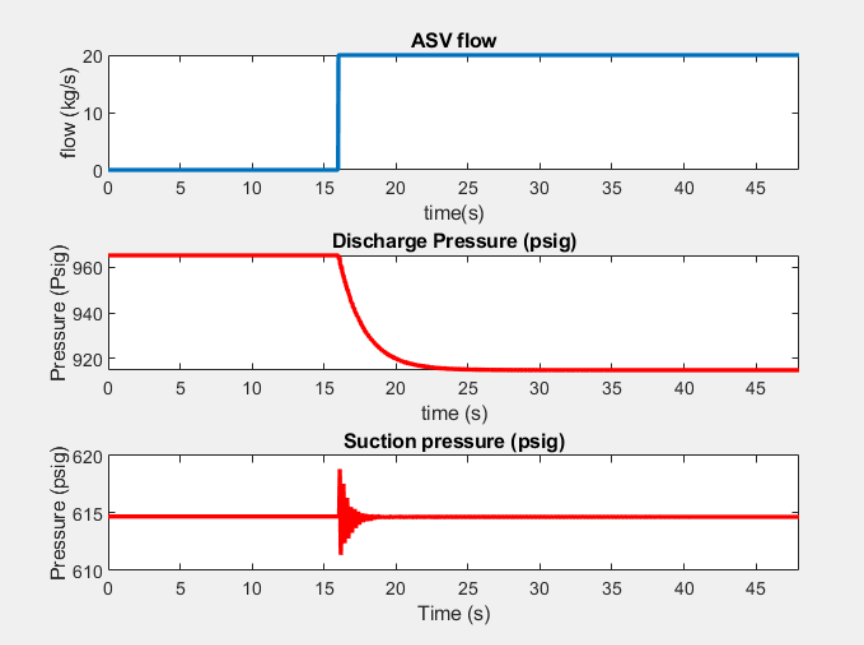

Figure 3.14 Step responses to ASV flow for packed midstream application

The behavior in Figures 3.9 and 3.10 can be described in a similar manner to that observed from Figures 3.7 and 3.8.

- Suction pressure does not change with either of the control signals but there is some oscillation.
- This resonance is the result of the constant tank pressure forcing the inlet (and consequently the suction pressure) to remain constant without any change in the flow rate through the system since the outlet pressure ($q_{6,r}$)is held constant.
- The discharge pressure drops to a lower value than it did for both the input changes (compared to a smaller tank volume) since the suction pressure cannot change.

3.7.2 Compressor performance curves

To test the validity of the model further, simulations were run at various compressor speeds for different mass flow rates through the ASV to map the pressure ratio from discharge to suction.

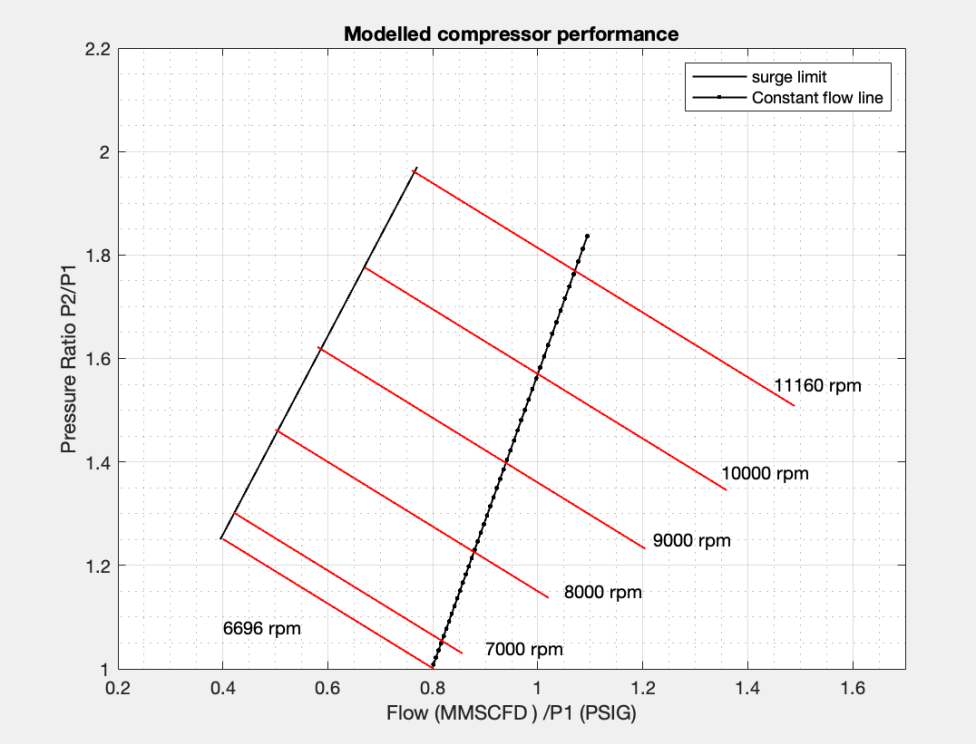

Figure 3.15 Recreated compressor performance curves

Figure 3.11 shows how the pressure ratio changes for different mass flows through the compressor at different speeds. This is a linearized version of the compressor performance curves from Figure 3.2 and is described by (2). The individual performance curves for each rpm match with the real compressor performance from Figure 3.2 close to the point of linearization (1 MMSCFD/P1, 1.575) but deviates significantly further away from it due to the approximation errors from linearization.

The constant flow line shows the trend followed by the compressor when the flow is kept constant while the speed is changed from the point of linearization (10,000 rpm). This line is not parallel to the vertical axis because the suction pressure now changes with the compressor speed. This linearized version of the compressor

performance curves shows that the compressor behaves as expected when interconnected with the rest of the model.

3.8. Anti-Aliasing filters and model reduction

A 38^{th} order system is constructed by concatenating the continuous time model of the interconnected system with two 8^{th} order[3] Butterworth Anti-Aliasing Filters (AAF's) with a cutoff frequency of 0.5 Hz (3.14 rad/s) on the measured signals suction ($p_{3,r}$) and discharge ($p_{5,l}$) pressures. AAFs are needed to move from a continuous-time system to a sampled-data system and then to discrete time for implementation of the digital controller. The continuous time model of the plant outputs continuous time signals which need to be sampled for a digital controller to be implemented. The controller is focused on the bulk gas flow and not the acoustics that may occur in the pipes. The AAF's get rid of the high frequency resonances before the signal is sampled.

Since we move from continuous time to discrete time via sampling, the AAFs are tied to the sampling time. The sampling time for gas pipeline systems are typically slow, usually at 1 Hz, so the cutoff frequency for the AAFs is chosen to be smaller than half the sampling frequency. Here we choose it to be 0.4 Hz = $0.8\pi \approx 2.513$ radians per second.

[3] While 8^{th} order might seem too high, this can be fixed in the next step of model reduction.

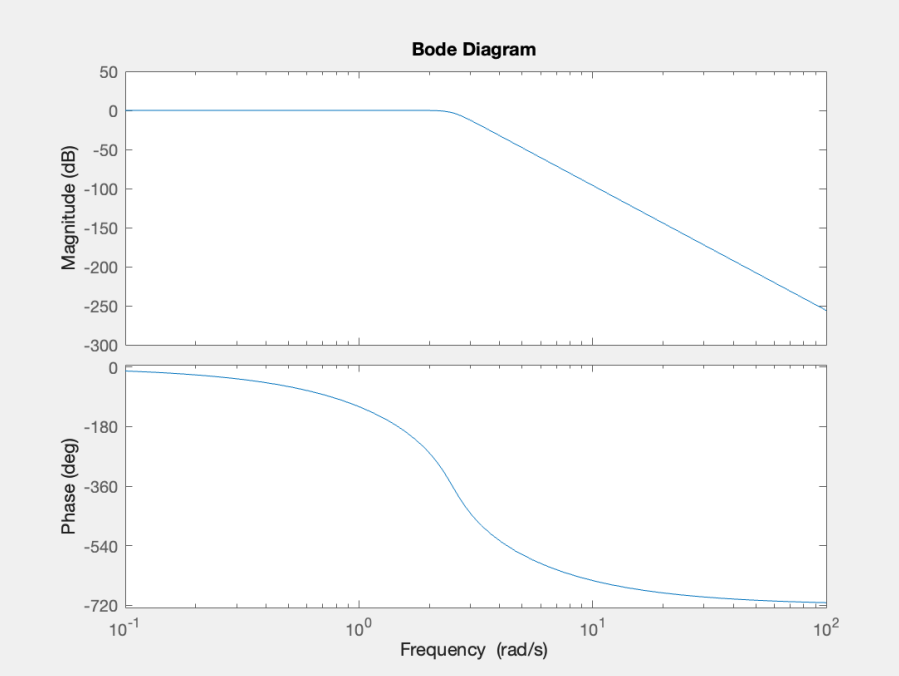

Figure 3.16 Frequency response of the AAF with cutoff frequency at pi rad/s and -3Db roll off at 0.8π rad/s for a sampling frequency of 2π rad/s.

Model reduction is then performed on the model with the AAFs to reduce the order. The idea of model reduction is that if the available model of a system is too complex for control design, remembering that poorly controllable or observable states may be connected with large gains within the controller, it is useful to reduce the model order while preserving the approximate input/output relationship. Balanced truncation is a form of model order reduction where the states are first transformed to have identical diagonal observability and controllability Gramians – this is 'balanced' – and then states with small values of controllability or observability are removed from the system. These states have a diminished effect on the input/output transfer function of the system. Thus removing these states does not overly affect the system behavior.

The resulting balanced realization of the model has equal and diagonal reachability and observability Gramians, with the non-negative elements on the main diagonals. These main diagonal elements are the Hankel singular values of the system and are listed in decreasing order. These values provide a measure of the contribution of each state to the transfer function, allowing states with very low singular values to be eliminated without great effect on the input output behavior.

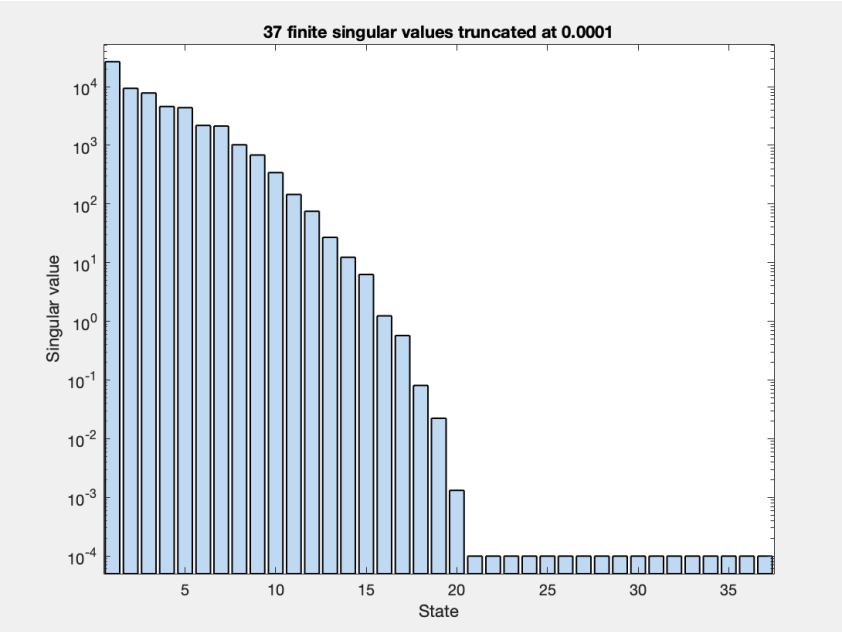

Figure 3.17 Hankel singular values of the stable modes for the 38th order system

The 38th order interconnected system (22nd order system (30) combined with two 8th order AAFs) is reduced to a 15th order system based on the Hankel singular values. The reduced model is described by the following system:

$$\dot{x} = A_r x + B_r u,\ y = C_r x + D_r u \tag{31}$$

Where A_r, B_r, C_r and D_r are the reduced system matrices

MATLAB™'s *'balreal'* function is used to compute a balanced state space realization and obtain the Hankel singular values. Then the '*modred'* function is used to reduce the model order by eliminating unwanted states and using the '*truncate'* option ensures that the strictly proper full order model results in a strictly proper reduced order model. Balanced truncation, since it requires computing Gramians, is only defined for strictly stable systems, i.e., poles inside the open left-half s-plane as the Hankel singular values do not exist for unstable poles. The interconnected system has one unstable pole at 0 because of the tank being modelled as an integrator and is thus left invariant. In Matlab's '*balreal*' function, unstable poles/states are isolated, balanced truncation is performed on the stable part, and then added back to the balanced and reduced stable part. The unstable part is unaffected by the model reduction. Figure 3.13 shows the Hankel singular values of the full order system with the anti-aliasing filters. There are 37 values associated with the stable modes plus the unstable integrator which is excluded from the reduction.

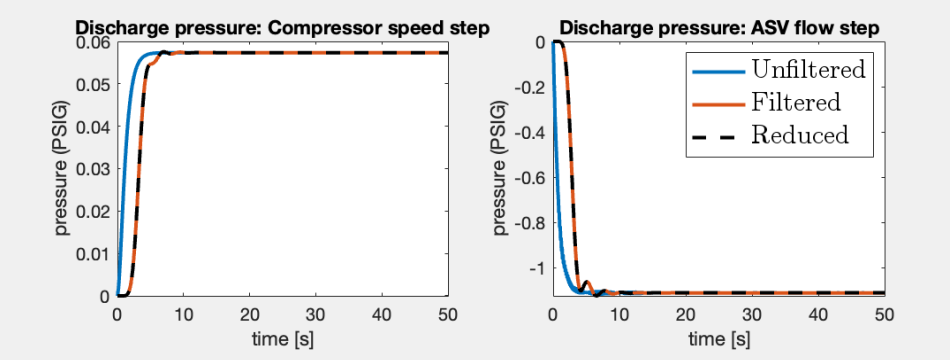

Figure 3.18 Discharge pressure step response to compressor speed and valve flow, comparison between loop system without AAF (unfiltered), with AAF (filtered), and with AAF and subsequent reduced order model (reduced).

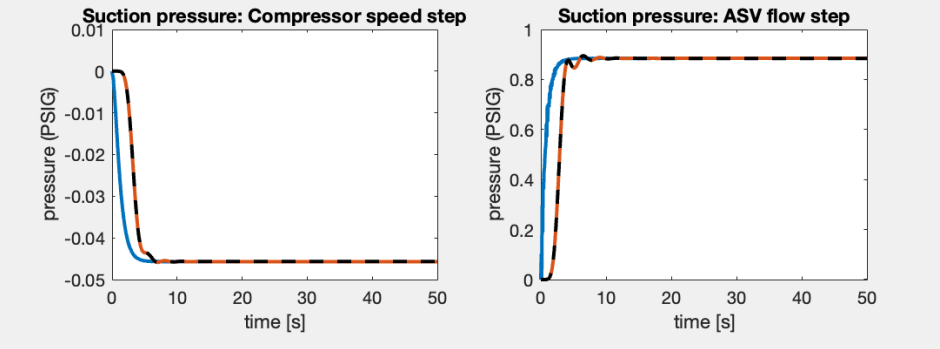

Figure 3.19 Suction pressure step response to compressor speed and valve flow, comparison between loop system without AAF (unfiltered), with AAF (filtered), and with AAF and subsequent reduced order model (reduced).

The step responses for the unfiltered and filtered full order models and the reduced 15th order models are compared in Figures 3.14 and 3.15.

- Firstly, the reduced order model approximates the full order model very well, as seen by the fact that the dashed black line perfectly matches the solid red line.
- Secondly, the AAFs introduce a phase delay to the signals, delaying the time at which the step response occurs.

Chapter 4 Model Based Control

The control design is performed in two stages with the end goal being the implementation of a digital controller. A continuous time controller is first designed since the plant model is already described in continuous time. The reduced order plant model is then converted to discrete time via Matlab's '*c2d*' function to design a discrete time controller. The output of this discretize controller is passed through a zero-order hold so it can used for the full order continuous time system.

4.1. Feedback design

Two LQG regulators are designed to control the suction and discharge pressures individually using the two control inputs. Linear-Quadratic-Gaussian (LQG) control is a fairly well understood modern state-space technique for designing dynamic regulators via an optimizing procedure. It enables the tradeoff between regulation and control effort while considering process disturbances and measurement noise to design a regulator of the same order as that of the system. The LQG regulator consists of an optimal state-feedback gain and a Kalman state estimator.

i) Optimal feedback regulator

The optimal state -variable feedback gain K for a system with state x and state equation:

$$\dot{x} = Ax + Bu, \tag{29}$$

Is computed by solving the Continuous time Algebraic Riccati Equation (CARE) for X:

$$0 = A^H X + XA - XBR^{-1}B^H X + Q, \;\; K = R^{-1}B^H X \tag{30}$$

Subject to the minimization of the cost function :

$$J_1 = \int_0^\infty (x^\dagger Q x + u^\dagger R u) dt \quad (31)$$

Resulting in the control law $u(t) = -Kx(t)$ (32)

Where Q and R are the costs associated with the states and inputs respectively

ii) Kalman Estimator

The LQ-optimal state feedback (17) is not implementable without full state measurement. When process and disturbance noises are included, it is possible.

$$\dot{x} = Ax + Bu + w, \qquad y = Cx + v.$$

However, to derive a state estimate $\hat{x}$ such that

$$u(t) = -K\hat{x}(t) \quad (33)$$

Remains optimal for the output-feedback problem with noises included. This state estimate is generated by the Kalman filter:

$$\dot{\hat{x}} = A\hat{x} + Bu + L(y - \hat{y}), \quad \hat{y} = C\hat{x} \quad (34)$$

The observer gain L is found by solving the following algebraic Riccati equation for P:

$$0 = AP + PA^T - PC^T V^{-1} CP + W, \;\; L = -PC^T V^{-1} \quad (35)$$

subject to the minimization of the cost functions J_2,

$$J_2 = \int_0^T trace(P(t))dt = \int_0^T \mathbb{E}(\|x - \hat{x}(t)\|^2 dt \geq 0 \quad (36)$$

W and V parametrize the covariance of the state disturbance $w(t)$ and the measurement noise $v(t)$ respectively.

The design parameters when building an LQG regulator are the Q, R, W and V matrices. Adjusting the Q and R matrices result in adjusting the control gain K as they

define the trade-off between regulation (how fast $x(t)$ goes to zero) and control effort: large Q and small R would result in higher control gains. Similarly, adjusting the W and V matrices alter the observer gain L which affects the observer smoothing: large W and small V would yield faster, noisier state estimates, for example.

The feedback is described by describing the plant (32), observer (37) and the control law (36) individually.

Plant: $\dot{x} = Ax + Bu + w, \qquad y = Cx + Du + v$

Observer: $\dot{\hat{x}} = A\hat{x} + Bu + L(y - \hat{y}), \qquad \hat{y} = C\hat{x}$

Control law: $u = -K\hat{x}$

Substituting (18) in (14) and (15) and replacing $\hat{y}$ with $C\hat{x}$ in (19) results in:

Plant: $\dot{x} = Ax - BK\hat{x} + w, \qquad y = Cx + Du + v$ (39)

Observer: $\dot{\hat{x}} = (A - BK - LC)\hat{x}, \qquad \hat{y} = C\hat{x}$ (40)

Which is the complete description of the feedback connection.

The reduced 15th order model is used to design individually two regulators (one for suction pressure and one for discharge pressure) using MATLAB's *'lqg'* function. the reduced order model is used for regulator design and the full order models because poorly controllable or observable states in the full order model may be connected with large gains within the controller, and the resulting controller will be of the same large order as well. Thus, each regulator is a 15th order system that has one input (suction or discharge pressure) and two outputs (commanded compressor speed and commanded ASV flow) and are then used to control the full 38th order system (22nd order interconnected system plus two 8th order AAFs)

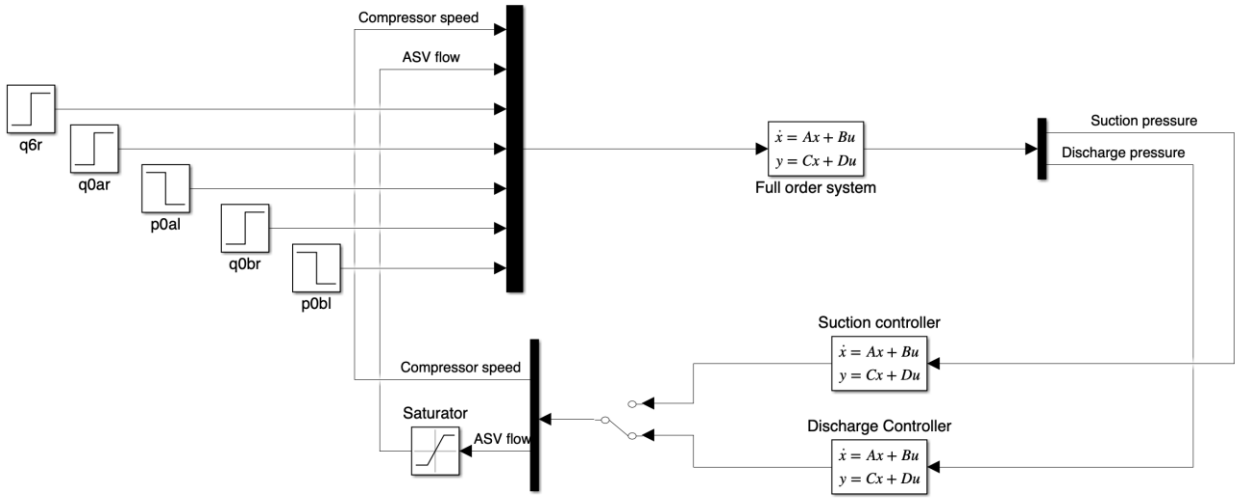

Figure 4.1 Feedback loop with individual LQG controllers for suction and discharge pressure regulation.

4.2. Simulations

Optimal control design varies parameters Q, R, W, V in the two Riccati equations (30) & (35) to yield gains K and L. There is significant redundancy in the choice of these parameters, but stabilization of the model is assured for any choices. A succession of designs was performed and these pairs of parameters (Q, R) and (W, V) adjusted to affect the closed-loop response.

Choosing $Q = {C_r}^T C_r$ allows the weighting to be placed directly on the output variables while also making it positive semidefinite. For the W and V matrices, since the SI unit for pressure is Pa, which is in the orders of approximately 10^5, versus kg/s for flow in the order of 10^1 general idea is to put more relative weight on the pressure while considering the units. One way to achieve this is to normalize the weights using the steady state pressures/flows. The covariance for the disturbance inputs (W) is chosen to be $B_r {B_r}^T$ to ensure that the off-diagonal elements of the covariance matrix are zero,

indicating no correlation between different components of the process noise and the measurement noise. Covariance (V) is normalized using steady state pressure. Notice that the emphasis is not on optimality but on using optimization for control design.

To test the controllers, a step disturbance in the upstream (source) pressures was simulated.

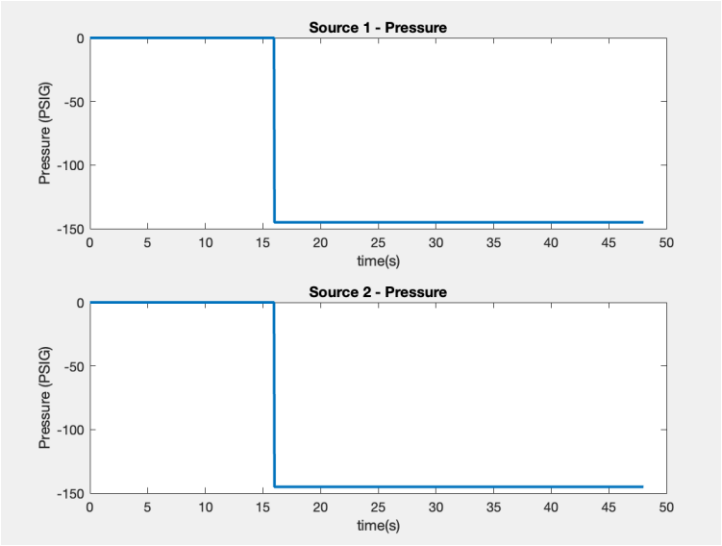

Figure 4.2 Step decrease in upstream pressures.

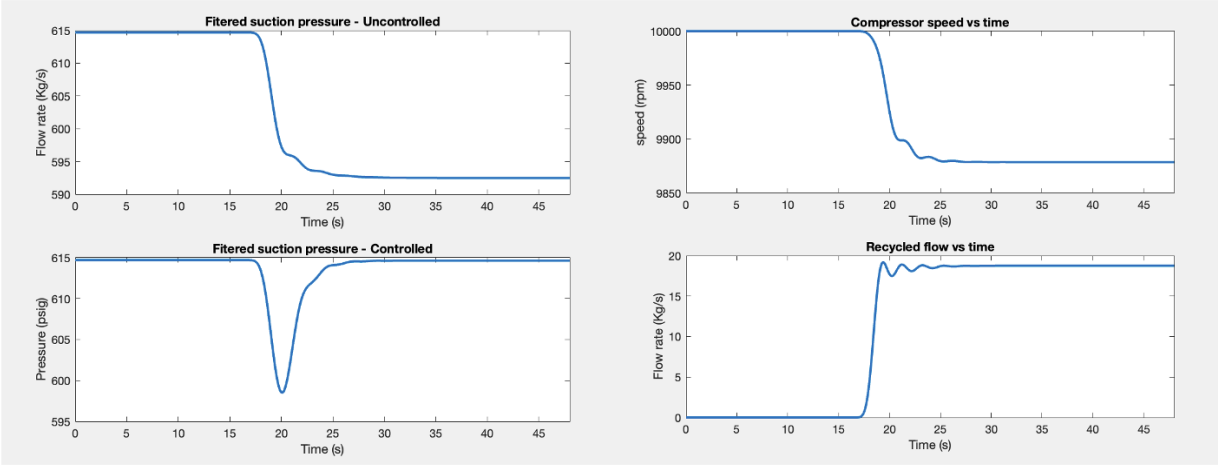

Figure 4.3 Suction pressure controller performance for decrease in upstream pressures.

- A decrease in upstream pressures causes a drop in suction pressure.
- Compressor speed decreases and flow is recycled from the discharge side to the suction side through the ASV to bring the suction pressure back to its set point.

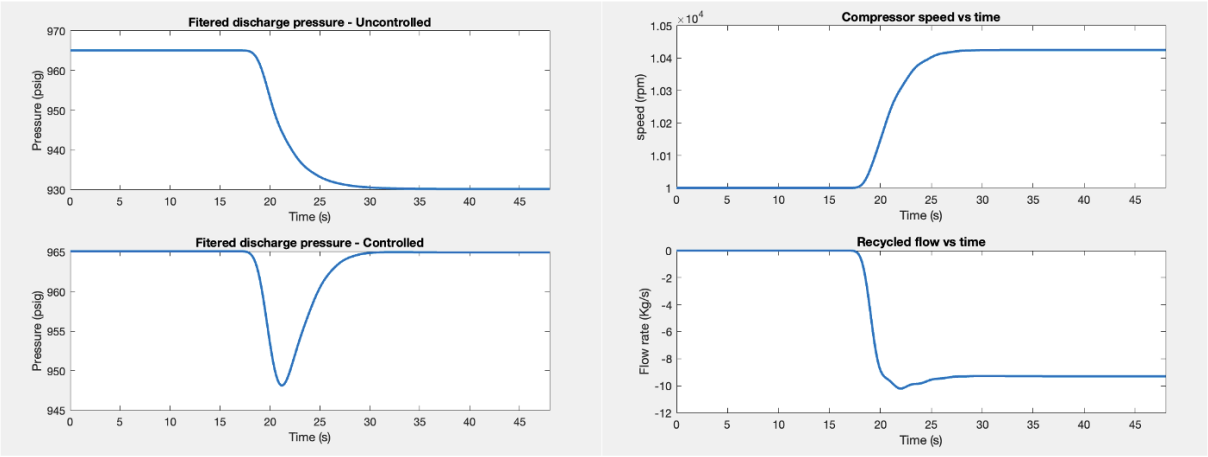

Figure 4.4 Discharge pressure controller performance for decrease in upstream pressures.

- A decrease in upstream pressures causes a drop in discharge pressure.
- Compressor speed increases along with a negative flow (from the low pressure suction side to the high pressure discharge side) through the ASV to bring the discharge pressure back to its set point.

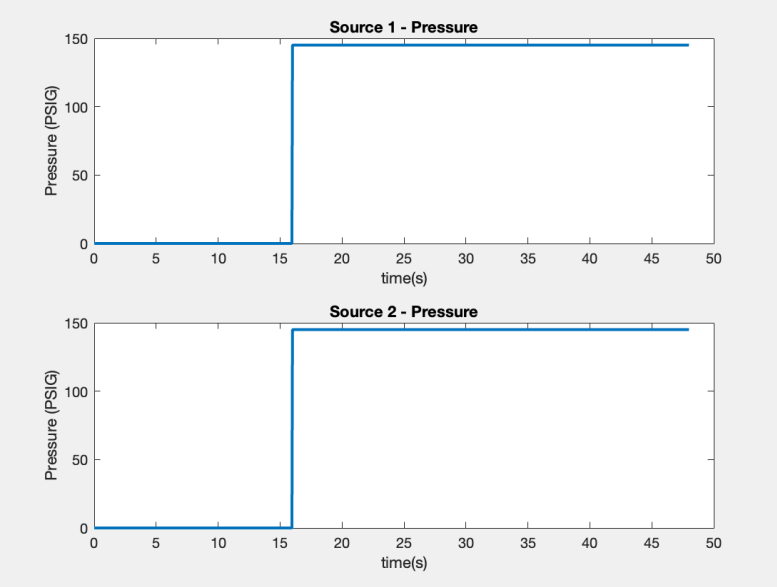

Figure 4.5 Step increase in upstream pressures.

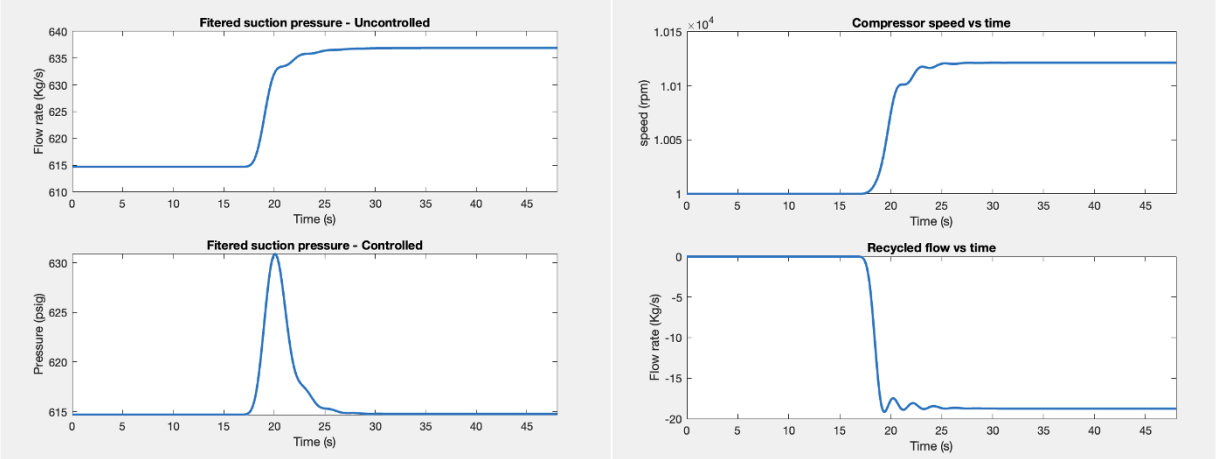

Figure 4.6 Suction pressure controller performance for increase in upstream pressures.

- An increase in upstream pressures causes a rise in suction pressure.
- Compressor speed increases along with a negative flow (from the low-pressure suction side to the higher pressure discharge side) through the ASV to bring the suction pressure back to its set point.

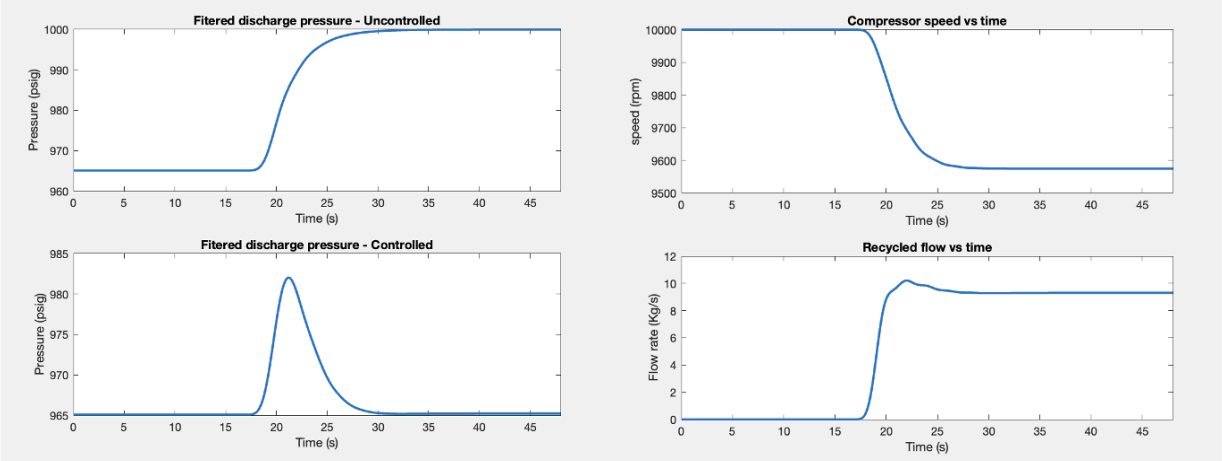

Figure 4.7 Discharge pressure controller performance for increase in upstream pressures.

- An increase in upstream pressures causes a rise in discharge pressure.
- Compressor speed decreases and flow is recycled from the discharge side to the suction side through the ASV to bring the discharge pressure back to its set point.

The controller built from the 15th order reduced model is capable of stabilizing the full order plant model. However, in the cases of an increase in suction pressure or decrease in discharge pressure as in Figures 4.5 and 4.6, there is negative flow through the ASV, which means the respective controller, although fulfilling its purpose of regulating suction or discharge pressure, is commanding gas to be sent from the low-pressure suction side to the higher-pressure discharge side, which cannot physically happen in the real world. The reason for this negative flow command is the lack of pressure as an input to the valve. The valve model simply removes and adds flow from its inlet and discharge sides respectively without consideration of which direction flow can be permitted as a consequence of pressure differences.

It can also be seen that in all cases that the ASV recycles flow, it remains open letting gas through as long as the disturbance exists in order to keep regulating the necessary pressure. Since

gas is always being recycled to maintain the set point, the system is in a state of partial recycle, which is a waste of the compressed gas.

4.3. Improved Feedback design

Two improvements are added to the feedback design to address the problems in the first simulation. Firstly, the integral of the ASV flow is added as an extra state (and output) to the model and is treated as an output to be controlled. The integral of the ASV flow represents how long the valve stays open, and the longer it stays open the higher the penalty imposed on it. This forces the controllers to close the valve in order to minimize it.

Secondly, the flow through the ASV is saturated to ensure there in no flow in the reverse direction through the valve. Because the valve model does not use any pressure signals as inputs, saturation prevents the valve model from having a negative flow (from the low-pressure suction side to the high-pressure discharge side), since that would not be physically possible. The saturation is not expressly included in the control design however, thus a lower limit of 0 kg/s of flow is placed on the ASV flow signal.

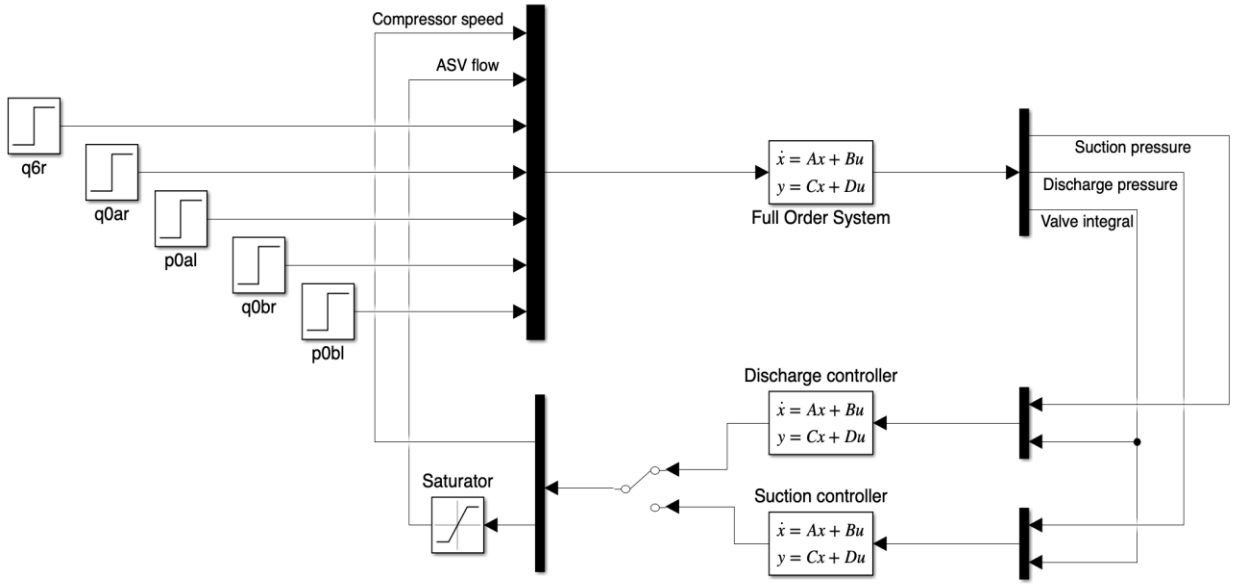

Figure 4.8 Improved feedback design with individual LQG controllers for suction and discharge pressure regulation.

4.3.1 Simulations

The same scenario (step disturbances in upstream pressures) is simulated with the new improved feedback design.

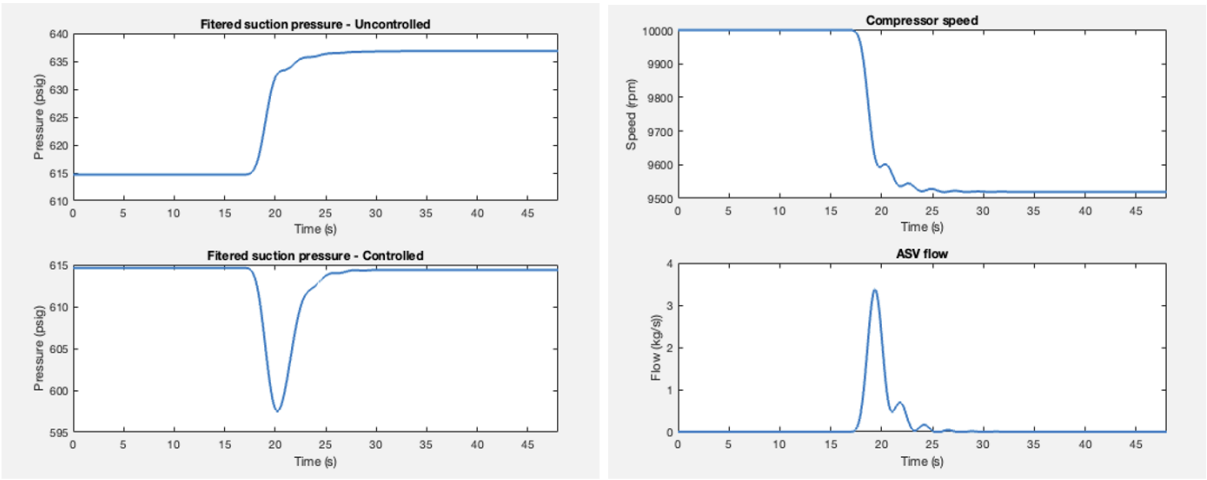

Figure 4.9 Improved suction pressure controller performance for decrease in upstream pressures.

- A decrease in upstream pressures causes a drop in suction pressure.
- Compressor speed decreases and flow is recycled from the discharge side to the suction side through the ASV to bring the suction pressure back to its set point.

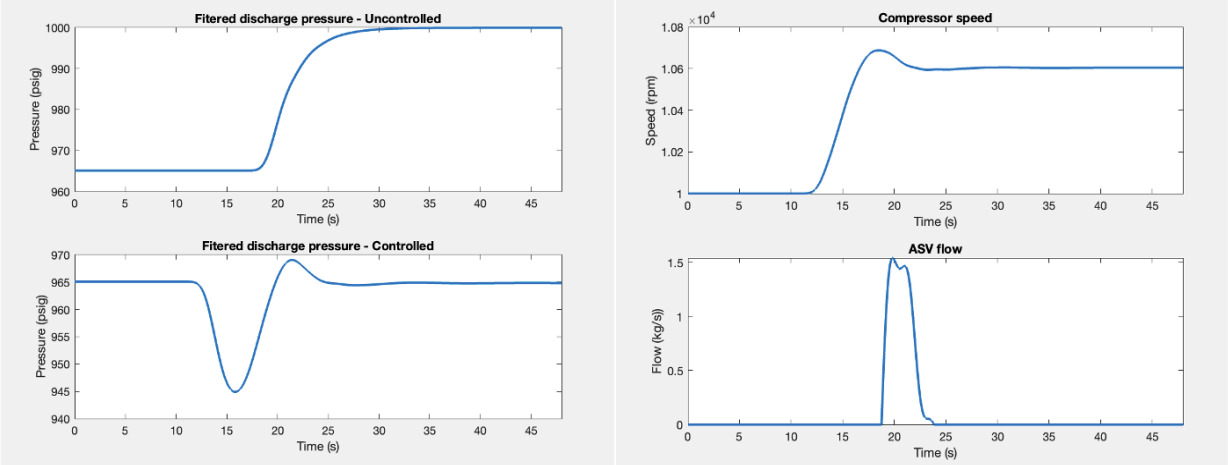

Figure 4.10 Improved discharge pressure controller performance for decrease in upstream pressures.

- A decrease in upstream pressures causes a drop in discharge pressure.
- The bulk of the control is expected to be done only by the compressor, since any recycling of flow will cause discharge pressure to decrease.
- Compressor speed increases with a slight overshoot, and a small amount of flow is recycled to bring the discharge pressure back to its set point.

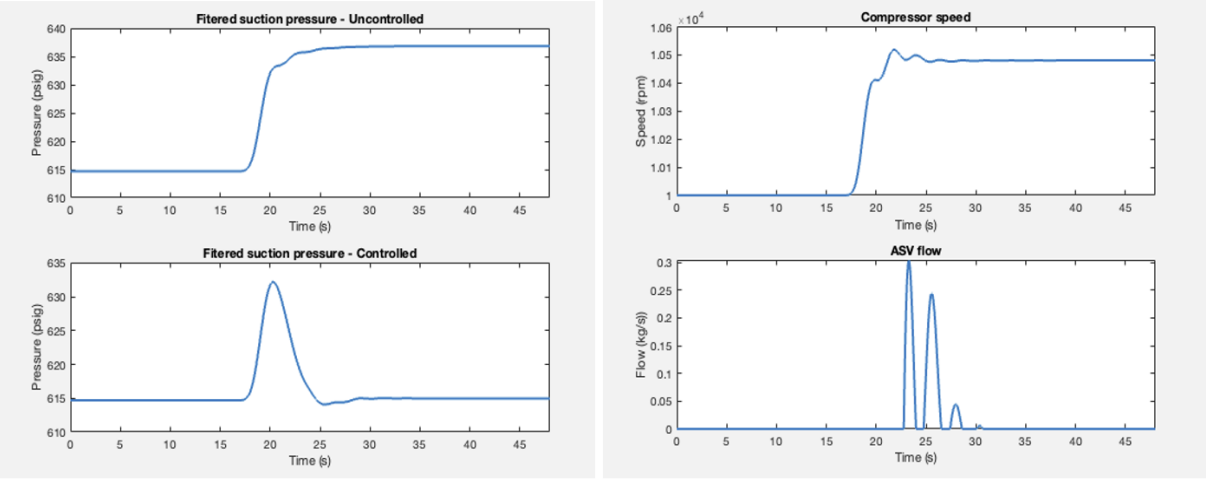

Figure 4.11 Improved suction pressure controller performance for increase in upstream pressures.

- An increase in upstream pressures causes an rise in suction pressure.
- The bulk of the control is expected to be done only by the compressor, since any recycling of flow will cause suction pressure to increase.
- Compressor speed increases with a slight overshoot, and a small amount of flow is recycled to bring the suction pressure back to its set point.

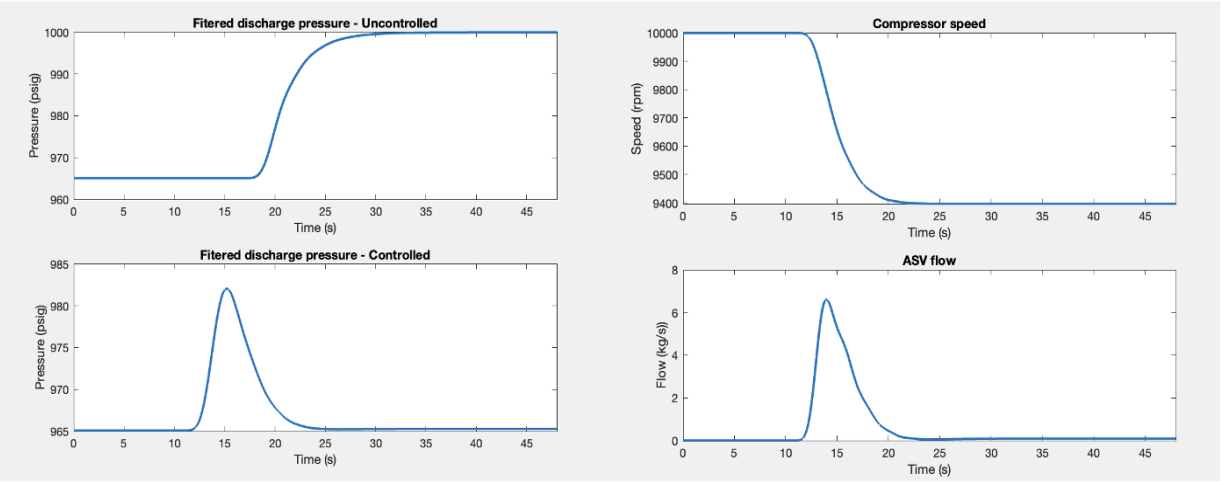

Figure 4.12 Improved discharge pressure controller performance for increase in upstream pressures.

- An increase in upstream pressures causes a rise in discharge pressure.
- Compressor speed decreases and flow is recycled from the discharge side to the suction side through the ASV to bring the discharge pressure back to its set point.

Having the integral of the valve as a state that is penalized, forces the valve to close after the controlled variable (suction/discharge pressure) reaches its set point. This ensures that the compressor system is no longer in a state of partial recycle and prevents the compressed gas from being wasted.

4.4. Modifying performance

The following parameters can be changed by changing the design parameters ($Q, R, W, and\ V$ matrices) of the controller:

1. Duration of recycle : The amount of time the ASV stays open can be adjusted by appropriately adjusting the cost on the output that represents the integral of the valve input.

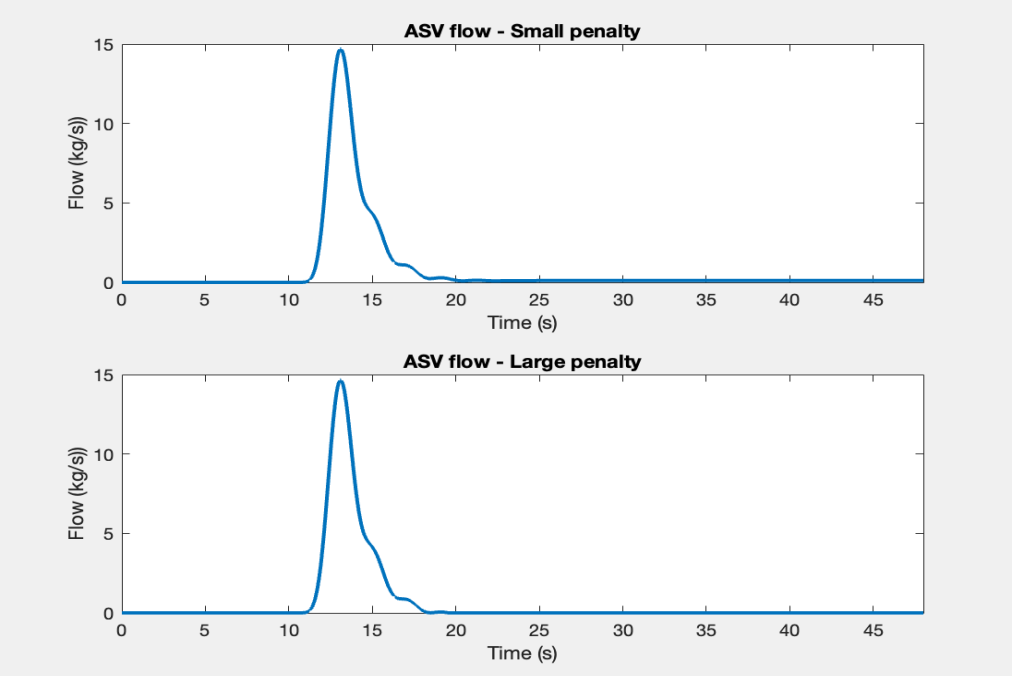

Figure 4.13 Effect of output penalty on ASV flow in regulating a decrease in suction pressure.

2. Amount of gas recycled : The quantity of flow recycled by the ASV can be changed by adjusting the cost on the valve input signal.

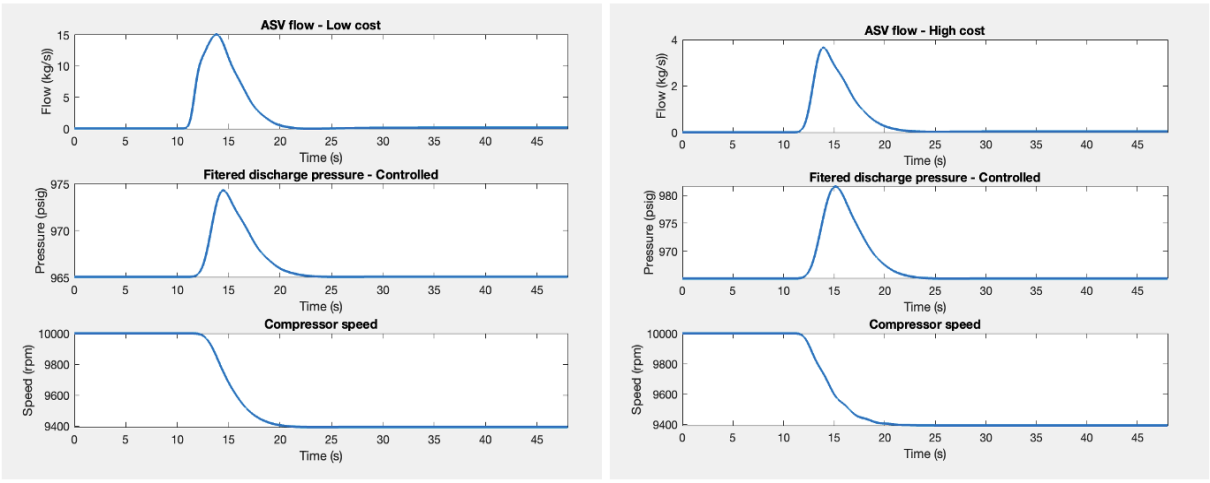

Figure 4.14 Effect of input cost on ASV flow in regulating an increase in discharge pressure.

The amount of recycled flow only affects how much the pressure rises before being controlled. In both cases, the compressor still reaches the same speed regardless of the amount of flow recycled since the valve must close eventually.

4.5. Discrete controller performance

In order to implement the controllers in discrete time, Matlab's '*c2d'* function is used to discretize the reduced (15^{th}) order model of the interconnected system. The same pairs of parameters (Q, R) and (W, V) chosen for the continuous time control design are used to design the discrete controller using the '*lqg'* function.

The same simulation (step disturbances in upstream pressures) in section 4.2 is used to test the discrete controllers.

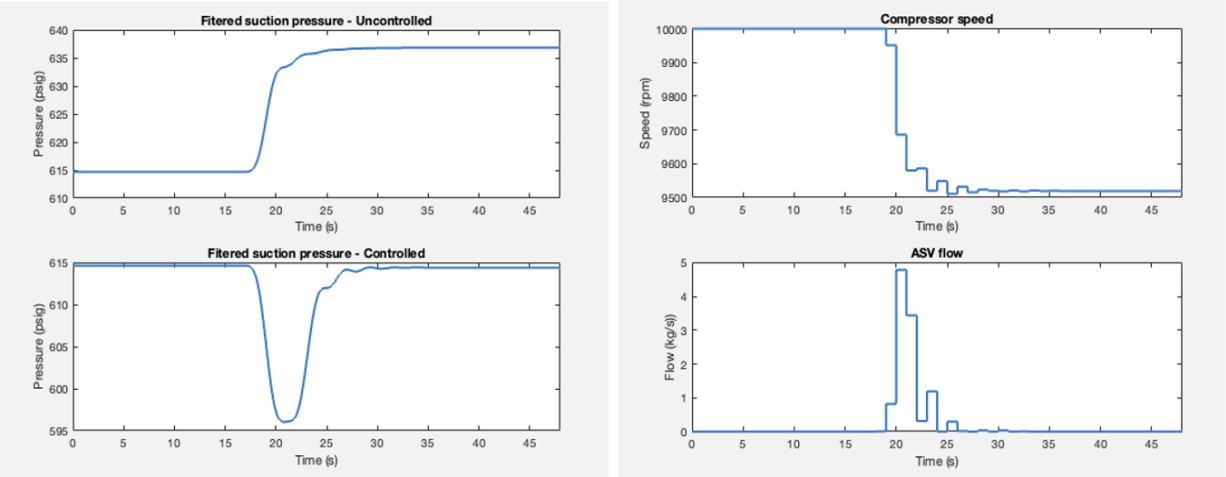

Figure 4.15 Discrete suction pressure controller performance for decrease in upstream pressures.

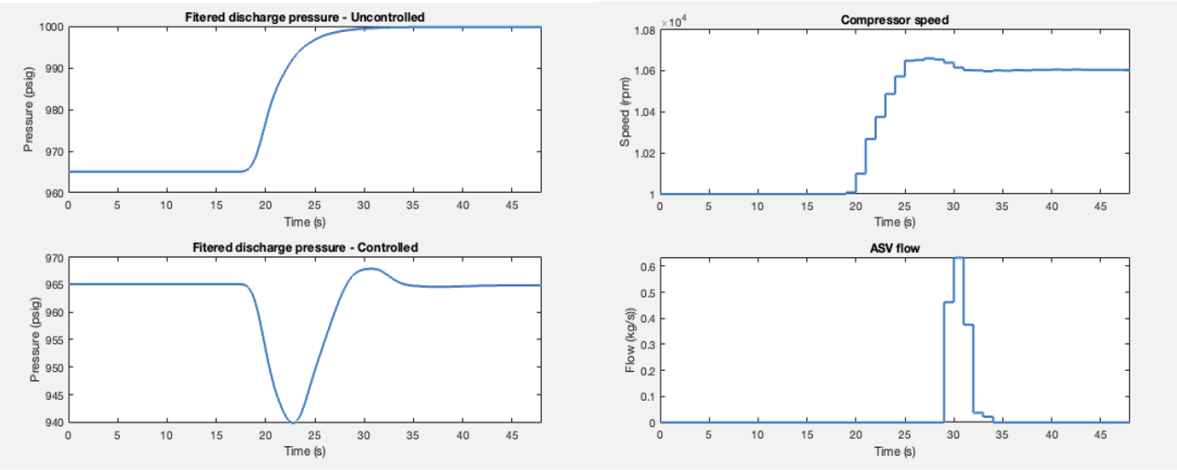

Figure 4.16 Discrete discharge pressure controller performance for decrease in upstream pressures.

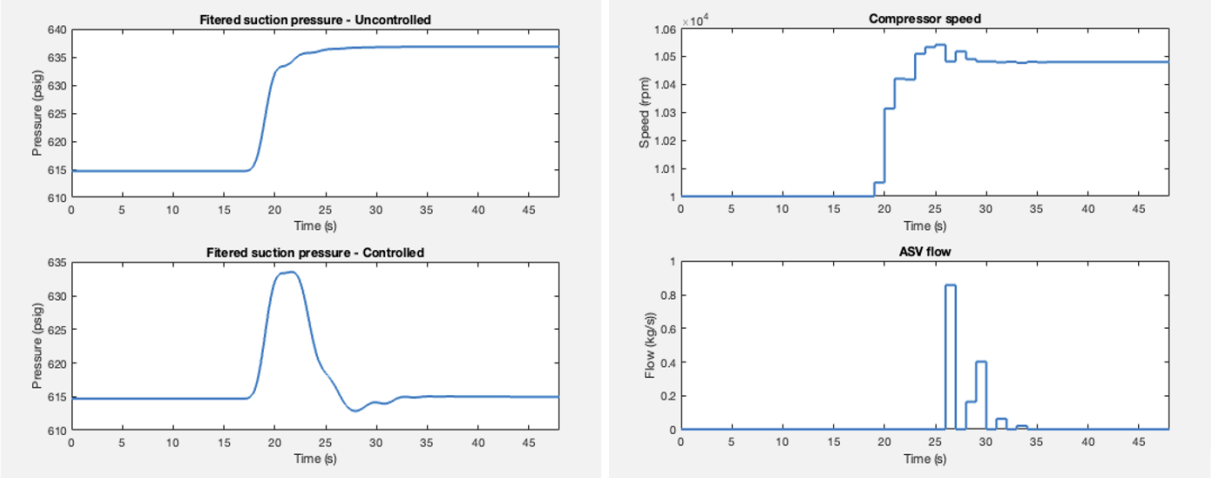

Figure 4.17 Discrete suction pressure controller performance for increase in upstream pressures.

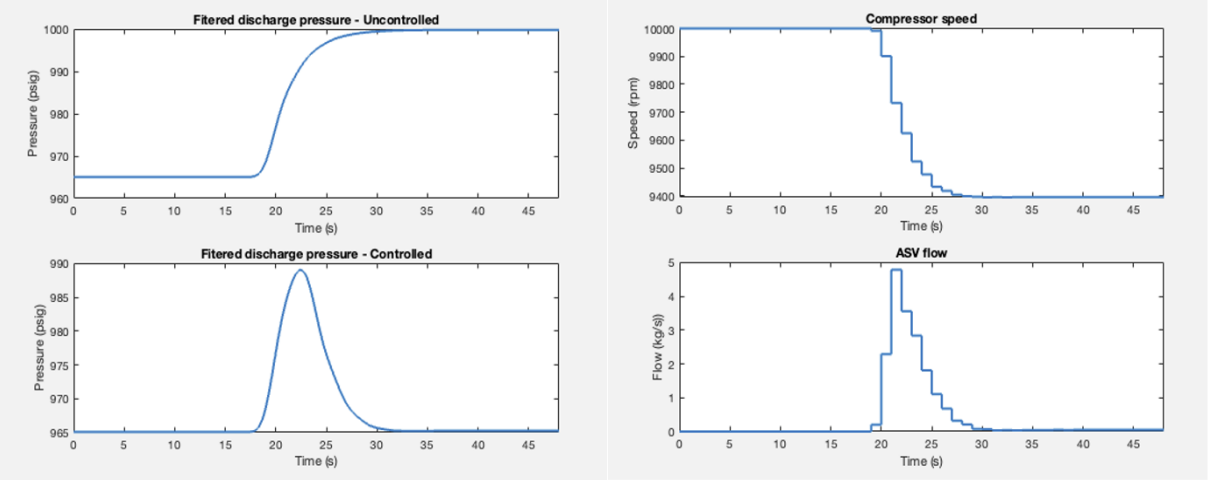

Figure 4.18 Discrete suction pressure controller performance for increase in upstream pressures.

Comparing the performance of the discretized controller to the continuous time controller (Figures 4.9, 4.10, 4.11, 4.12) we see that the discrete controller has similar performance but recycles a slightly different amount of flow. This discrepancy could be due to the fact that the discrete time controller was designed using a discretized model of the plant but is used for feedback control of the continuous time model of the plant.

Chapter 5 Conclusions and Future Direction

This work describes the development of control-oriented models for application in gas processing. The central features are that the accommodation of the physical operating environment and objectives drive the composition of the models and the control design in an orchestrated fashion. The models, while overtly highly simplified from their PDE antecedents, are shown to suit the feedback control methods of LQG, with their capacity for MIMO controllers including realistic operational parameters. The comparison methods are multiple single-channel PI controllers, for which design methods and guidance are wanting.

The required extension of component models from [2], [3], [4] and [5] was of particular importance and piquancy, in that the models needed adjustment for this new application purpose but also that this was achieved quite directly and without needing to exit the general framework of compartmentalized models.

As an example of the modeling-for-control paradigm, which is still awaiting a solid formalism, the results indicate the core feature of simplicity and the need for linearity in order to use familiar control design tools. They also reinforce the requirement for inclusion of the ultimate control objective into the evaluation of the model. Equally, the ad hoc nature of the accommodation of the nonlinearity of the valve flow is a clear limitation of the approach; perhaps it was just luck. However, side stepping the nonlinear valve control - aperture specification to resultant flow - appears to be a repeatable systematic method for avoiding (at least monotonic) nonlinear actuators.

The next natural phase is to implement and test these controllers in the field for more rigorous and practical evaluation. That is a stage which will require prototyping and safety-jacketing. The conclusions from the current analysis are that the capabilities promised are suitably attractive to warrant considering these next steps.

Avenues for further research could include the following. Starting with the control-oriented modelling, the choices for the states and inputs can be swapped when performing the spatial discretization of the continuity, momentum, and ideal gas equations in (2) i.e. having the state variables be identified with the pipe PDE boundary conditions, p_l, q_r and the input variables with the ODE solution, p_r, q_l. This exchange of variables could lead to all the

component inputs being connected to a component output when creating the interconnected system without a great deal of change in the state space matrices of the individual models.

The approach for control design used in this thesis is to build the low order controller using the lower order approximation of the plant model. An equally valid method would be to build a high order controller from the original full order plant model and then reduce its order. One might also consider directly developing a low order controller based on the full order plant model without a model reduction step.

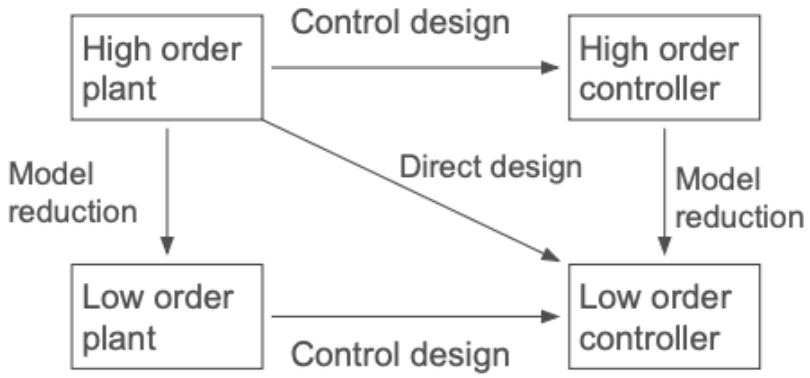

Figure 5.1 Different approaches to designing a low order controller for a full order plant.

The advantages and disadvantages of these different approaches are explored in [6]. Direct low order design in difficult since the extent to which iteratively tuning the weighting matrices (as is done for the conventional LQG design method) is possible or even how to do it is far from clear. The authors also reason that it should be more desirable to design a high order controller first and approximate it rather than the other way around with the general argument being that the approximation occurs as late as possible, minimizing the approximation errors.

The more specific reason is that since the low order controller is to be used in feedback with the full order control, any controller approximation demands knowledge of the plant in order to retain the same quality of performance. But this leads to a dilemma because the same argument applies to needing the controller information to obtain a faithful approximation of the plant model. A controller-suited plant model is needed to build an appropriate reduced model of the controller, while the associated controller-suited plant model would need to be connected to the reduced-order controller. This calls for iteration … and hope.

Nevertheless, it may be worthwhile to explore other approaches by including ideas from [6] where the control objective plays a central role in modifying the model reduction phase. This permits the replacement of balanced truncation by a more control-oriented approach, allowing the modeling, model reduction and control design each to reflect the closed-loop objectives. The same thing can be said about discretizing the plant to build a discrete controller vs discretizing a continuous controller.

The material in this thesis, in part, has been submitted for publication of the material as it may appear in the Conference for Control Technology and Applications, 2024, Ramadurai, Varun; Bitmead, Robert, 2024. The thesis author was the primary researcher and author of this paper.

```
%% Constants

psig2pa=6894.75728;          % Conversion from psig to pascal
mmscfd2kgps=0.55/2.2;        % conversion from mmscfd to kg/s
pbar_psig=650;               % nominal pipe pressure psig
pbar = pbar_psig*psig2pa;    % nominal pressure Pa
pbarVol = pbar*0.9;          % nominal pressure in large volume [Pa]
qbar = 614.7*mmscfd2kgps;    % nominal flow Kg/s
Re = 1.1684e8 ;              % 1.0901e7; % Reynolds number
T = 300;                     % nominal temperature K
z = 1;                       % gas compression factor
Rs = 518.28;                 % specific gas constant JK^{-1}mol^{-1} methane
lambda = 0.0113*1;           % friction factor
gamma = Rs*T;                % constant gas state
L = 10;                      % Pipe Length [m]
D = 27.25*2.54/100;          % Pipe Diameter [m]
A = pi*D*D/4;                % Pipe Cross-sectional area [m^2]

%% Sys1 : Joint 123 (Modelled as a branch)

% Pipe 1dc
D1 = 30*2.54/100;
A1 = pi*D1*D1/4;
q1bar=qbar;
alf1 = -gamma*z/A1/L;
bet1 = -A1/L;
kapp1 = A1/L + lambda*gamma*z*q1bar*abs(q1bar)/2/D1/A1/pbar^2;
gamm1 = -lambda*gamma*z*abs(q1bar)/D1/A1/pbar;
% Pipe 2 % (Assuming negative flow)
q2bar=-qbar;
D2=D;A2=A;
alf2 = -gamma*z/A2/(L/2);
bet2 = -A2/(L/2);
kapp2 = A2/(L/2) + lambda*gamma*z*(q2bar)*abs(q2bar)/2/D/A2/pbar^2;
gamm2 = -lambda*gamma*z*abs(q2bar)/D/A2/pbar;
% Pipe 3
D3 = 24*2.54/100;
A3 = pi*D3*D3/4;
q3bar=qbar;
alf3 = -gamma*z/A3/L;
bet3 = -A3/L;
kapp3 = A3/L + lambda*gamma*z*q3bar*abs(q3bar)/2/D3/A3/pbar^2;
gamm3 = -lambda*gamma*z*abs(q3bar)/D3/A3/pbar;
% Composite sys1 (J123)
```

```
delta123=alf2/(alf1+alf2);
Ajb=[0,0,0,-alf1,alf1,alf1;
0,0,0,0,-alf2,0;
0,0,0,0,0,-alf3;
bet1,0,0,gamm1,0,0;
kapp2,bet2,0,0,gamm2,0;
kapp3,0,bet3,0,0,gamm3];
Bjb=[0,0,0;
0,alf2,0;
0,0,alf3;
kapp1,0,0;
0,0,0;
0,0,0];
Cjb=[0,1,0,0,0,0;
0,0,1,0,0,0;
0,0,0,1,0,0];
Djb=zeros(3,3);
sys123_jb=ss(Ajb,Bjb,Cjb,Djb);
sys123_jb.u={'p1l','q2r','q3r'};
sys123_jb.y={'p2r','p3r','q1l'};
sys123_jb.StateName={'p1r','p2r','p3r','q1l','q2l','q3l'};

%% Sys2 : Branch 456

% Pipe 5
D5 = 24*2.54/100;
A5 = pi*D5*D5/4;
q5bar=qbar;
alf5 = -gamma*z/A5/L;
bet5 = -A5/L;
kapp5 = A5/L + lambda*gamma*z*q5bar*abs(q5bar)/2/D5/A5/pbar^2;
gamm5 = -lambda*gamma*z*abs(q5bar)/D5/A5/pbar;
% Pipe 6
D6 = 42*2.54/100;
A6 = pi*D6*D6/4;
q6bar=qbar;
alf6 = -gamma*z/A6/L;
bet6 = -A6/L;
kapp6 = A6/L + lambda*gamma*z*q6bar*abs(q6bar)/2/D6/A6/pbar^2;
gamm6 = -lambda*gamma*z*abs(q6bar)/D6/A6/pbar;
% Pipe 4
q4bar=qbar;
D4=D;A4=A;
alf4 = -gamma*z/A4/(L/2);
bet4 = -A4/(L/2);
kapp4 = A4/(L/2) + lambda*gamma*z*q4bar*abs(q4bar)/2/D/A4/pbar^2;
gamm4 = -lambda*gamma*z*abs(q4bar)/D/A4/pbar;
% Composite sys2 (B456)
```

```
Ab=[0,0,0,-alf5,alf5,alf5;
0,0,0,0,-alf4,0;
0,0,0,0,0,-alf6;
bet5,0,0,gamm5,0,0;
kapp4,bet4,0,0,gamm4,0;
kapp6,0,bet6,0,0,gamm6];
Bb=[0,0,0;
0,alf4,0;
0,0,alf6;
kapp5,0,0;
0,0,0;
0,0,0];
Cb=[0,1,0,0,0,0;
0,0,1,0,0,0;
0,0,0,1,0,0];
Db=zeros(3);
sys456_b=ss(Ab,Bb,Cb,Db);
sys456_b.u={'p5l','q4r','q6r'};
sys456_b.y={'p4r','p6r','q5l'};
sys456_b.StateName={'p5r','p4r','p6r','q5l','q4l','q6l'};

%% Sys3 : Compressor

kc = 1.57;
Ac = zeros(2,2);
Bc = zeros(0,3);
Cc = zeros(2,0);
Dc = [kc, -2.5*psig2pa, 8.9002e5/1000;  0,1,0];
sysC = ss(Ac,Bc,Cc,Dc);
sysC.u = {'p3r','q5l','w'};    % pCl=p3r, qCr=q5l
sysC.y = {'p5l','q3r'};        % qCl=q3r, pCr=p5l
sysC.StateName = {'pCr','qCl'};

%% Sys4 : EMD

tau=2;
num=tau;
den=[1 tau];
[Ad,Bd,Cd,Dd] = tf2ss(num,den);
sysM=ss(Ad,Bd,Cd,Dd);
sysM.u={'w_tau'};
sysM.y={'w'};
sysM.StateName={'w'};

%% Sys5 : Valve

Av = zeros(2,2);
Bv = zeros(0,3);
```

```
Cv = zeros(2,0);
Dv = [1,0,0;-1,0,0];
sysV = ss(Av,Bv,Cv,Dv);
sysV.u = {'q_u','p4r','p2r'};  % qVl=q4r, and qVr=q2r
sysV.y = {'q4r','q2r'};        % qVl=q4r, and qVr=q2r
sysV.StateName={'qVl','qVr'};

%% Source model

lambdap=lambda;
Lp0=250;
Diap0=9*2.54/100;
Arp0 = pi*Diap0*Diap0/4;
qp0bar = -qbar;
alfp0 = -gamma*z/Arp0/(Lp0);
betp0 = -Arp0/(Lp0);
kappp0 = Arp0/(Lp0)+lambdap*gamma*z*(qp0bar)*abs(qp0bar)/2/Diap0/Arp0/pbar^2;
gammp0 = -lambdap*gamma*z*abs(qp0bar)/Diap0/Arp0/pbar;
Ap0a=[0 -alfp0;
betp0 gammp0];
Bp0a=[0 alfp0;
kappp0 0];
Cp0a=eye(2);
Dp0a=0;
sysp0a=ss(Ap0a,Bp0a,Cp0a,Dp0a);
sysp0a.u={'p0al','q0ar'};
sysp0a.y={'p0ar','q0al'};
sysp0a.StateName={'p0ar','q0al'};

sysp0b=sysp0a;
sysp0b.u={'p0bl','q0br'};
sysp0b.y={'p0br','q0bl'};
sysp0b.StateName={'p0br','q0bl'};

Vvol = 1e1;

At=zeros(1,1);
Bt=(gamma*z/Vvol)*[1 1 -1];
Ct=1;
Dt=[0 0 0];
sys_t=ss(At,Bt,Ct,Dt);
sys_t.u={'q0al','q0bl','q1l'};
sys_t.y={'p1l'};
sys_t.StateName={'pt'};

inputs = {'q0ar','p0al','q0br','p0bl','q1l'};
outputs = {'p0ar','p0br','q0al','q0bl','p1l'};
source_model = connect(sysp0a,sysp0b,sys_t,inputs,outputs);
```

```
189
190     %% Interconnected system
191
192     inputs = {'speed','u','q6r','q0ar','p0al','q0br','p0bl'};
193     outputs = {'p2r','p3r','q1l','p4r','p6r','q5l','p5l','q3r','q4r', ...
194     'q2r','w','p1l','p0ar','p0br','qtl1','qtl2'};
195     total_sys = connect(sys123_jb,sys456_b,sysC,sysM,sysV, ...
196     source model,inputs,outputs);
```

REFERENCES

[1] Kurz, R., and Brun, K. (October 3, 2017). "Process Control for Compression Systems." ASME. *J. Eng. Gas Turbines Power*. February 2018; 140(2): 022401. https://doi.org/10.1115/1.4037723

[2] Brüggemann, Sven, Robert H. Moroto, and Robert R. Bitmead. "Control-Oriented Modeling of Pipe Flow in Gas Processing Facilities." *IEEE Transactions on Control Systems Technology* (2023).

[3] Brüggemann, Sven, Robert H. Moroto, and Robert R. Bitmead. "Control-orientation, conservation of mass and model-based control of compressible fluid networks." *arXiv preprint arXiv:2211.06826* (2022).

[4] Brüggemann, Sven, Robert H. Moroto, and Robert R. Bitmead. "A Compendium of Control-Oriented Models of Gas Processing Equipment Components." *arXiv preprint arXiv:2211.06813* (2022).

[5] P. Benner, S. Grundel, C. Himpe, C. Huck, T. Struble, and C. Tischendorf, "Gas network benchmark models," in *Applications of Differential-Algebraic Equations: Examples and Benchmarks* (S. Campbell, A. Ilchmann, V. Mehrmann, and T. Reis, eds.), pp. 171– 197, Springer Nature, 2018.

[6] Obinata, Goro, and Brian DO Anderson. *Model reduction for control system design*. Springer Science & Business Media, 2012.

[7] Department of Electrical and Computer engineering, Northwestern University. (n.d.). Designing compensators (getting started). http://www.ece.northwestern.edu/local-apps/matlabhelp/toolbox/control/getstart/desig31a.html

[8] Middleton, Richard H. "Trade-offs in linear control system design." *Automatica* 27.2 (1991): 281-292

[9] Bewley, Thomas. "*Numerical renaissance: simulation, optimization and control* " First edition (hardbound, English language), 2018. ISBN # 978-0-9818359-0-7.